Journal of
Polymer Materials

Tech Science Press

https://doi.org/10.32604/jpm.2026.074982

REVIEW

Influence of Key Parameters on the Crack Growth Resistance Curve (R-Curve) Behavior of End-Notched Flexure (ENF) Specimens of Laminated Composites: A Review

Mazaher Salamat-Talab[1,*], Hossein Kazemi[1,2] and Mehdi Safari[1]

[1]Department of Mechanical Engineering, Arak University of Technology, Arak, Iran
[2]School of Mechanical Engineering, Iran University of Science and Technology, Tehran, Iran

*Corresponding Author: Mazaher Salamat-Talab. Email: salamattalab@arakut.ac.ir

Received: 22 October 2025; Accepted: 09 April 2026; Published: 30 June 2026

ABSTRACT: Polymeric composite laminate materials have gained a prominent position in advanced industries because of their outstanding mechanical, thermal, and chemical properties. However, the lack of through-thickness reinforcement and the stress inconsistencies at the fiber-matrix interface result in weak out-of-plane properties and increase the delamination likelihood. Delamination is often a concealed form of damage that significantly diminishes the mechanical properties and long-term durability of laminated composites. Therefore, it is essential to recognize that, due to the significant shear stresses encountered in practical applications, a thorough understanding of delamination behavior under mode II loading is necessary. Also, this understanding cannot be achieved without a detailed analysis of the crack growth resistance curve (R-curve). Therefore, this review, in the first place, provides a comprehensive overview of the theoretical background and significance of the R-Curve in the mode II condition and analyzes the standard experimental methods and commonly used data reduction models, i.e., compliance calibration method (CCM) and the compliance-based beam method (CBBM), which are developed to determine this curve. Following this, conventional approaches to improving delamination resistance in laminated composites, such as stitching, Z-pinning, matrix toughening, and fiber surface treatment, are discussed, emphasizing their respective advantages and disadvantages. Afterwards, the review focuses on more efficient strategies to improve the R-Curve of laminated composites, specifically through modifications in stacking sequences and, most notably, the use of interlayers. Overall, the review of related studies indicated that incorporating optimized interlayers, especially hybrid or specially structured types, can significantly improve mode II ILFT, resulting in fully rising R-Curves. It should be noted that the primary goal of all strategies is to enhance the mode II ILFT by increasing the interaction and friction between layers in laminated composites. This improvement enables various toughening mechanisms to work together, including fiber bridging, fiber breakage, crack pinning, and crack arresting.

KEYWORDS: Composite laminate materials; crack growth resistance curve; delamination; interlayer; mode II interlaminar fracture toughness

1 Introduction

Composite materials are a specialized category of advanced materials formed by combining two or more components, each exhibiting distinct properties. The primary objective behind the development of composite materials is to achieve a specific set of properties that cannot be realized by any individual component alone [1]. It is worth noting that over the past few decades, this approach has positioned composite materials as vital materials across various industries [2,3]. Typically, the components of a composite

material can be categorized into two phases: the matrix phase and the reinforcing phase [1], which, based on these phases, composites are classified into several major groups. For instance, based on the type of matrix material used, composite materials are generally categorized into three main types: polymer matrix composites (PMCs, which are valued for their ease of processing and high strength-to-weight ratio) [4,5], metal matrix composites (MMCs, known for their applications in high-temperature environments and their excellent wear resistance) [6,7], and ceramic matrix composites (CMCs, which are distinguished by their ability to withstand extremely harsh thermal and corrosive conditions) [8,9]. It should be noted that, among these, PMCs are the most common type of composite materials, primarily due to their unique advantages and cost-effectiveness [5,10]. Additionally, within the broader category of PMC materials, there are further classifications based on the size of the reinforcement (micro or nano) and the type used, resulting in materials such as nanocomposites and laminated composites. In this field, although nanocomposite materials possess attractive mechanical [11–13], thermal [14,15], and chemical properties [16,17], their widespread use is often limited by structural challenges during manufacturing [18–20], as well as concerns related to cost and biocompatibility [21–23]. In contrast, laminated composite materials have gained popularity and widespread acceptance in various industries due to their distinct advantages and broad range of applications across different fields [24–26].

In polymeric laminated composite materials, fibers act as the primary load-bearing elements, while the resin serves as the binding matrix that holds them together. In fact, this combination creates a structure that is lightweight, strong, and flexible [4,5,10]. One of the key advantages of these materials is their design flexibility and the simplicity of fabrication, further enhancing their appeal [27]. In addition to these benefits, laminated composite materials offer a high strength-to-weight ratio, excellent corrosion resistance, and the ability to be molded into complex shapes, all of which significantly contribute to their popularity [27,28]. These qualities have made laminated composites effective alternatives in various industries, including aerospace, marine engineering, automotive manufacturing, and even sporting equipment. Nevertheless, despite these advantages, laminated composite materials are not without limitations [28]. For instance, a significant challenge is their susceptibility to out-of-plane loading due to inherent heterogeneity and discrepancies in mechanical, thermal, and chemical properties between the matrix and the reinforcement in these materials [29]. These circumstances can lead to stress concentrations and uneven stress distributions at the interlaminar interfaces, resulting in delamination, the gradual or sudden separation of adjacent layers in laminated composite materials [29].

Delamination is recognized as one of the most critical types of damage in laminated composite materials. It poses a significant failure by drastically reducing load-bearing capacity and stiffness, and it often develops without any visible warning signs before a catastrophic failure occurs [30–32]. Delamination damage typically begins when mechanical or thermal loading weakens the bond at the matrix-fiber interfaces in laminated composites, leading to discontinuities and microcracks at the interlaminar regions [33,34]. This fact means that in safety-critical structures, such as aircraft or ships, even a small, imperceptible interlaminar crack can escalate into irreparable damage. It should be noted that factors such as insufficient matrix-fiber contact, the presence of voids or impurities, and mismatches in the coefficients of thermal expansion among the laminated composite materials can accelerate this process [35,36]. As a result, it has become one of the key research challenges in this field [28]. Therefore, since the late twentieth century, numerous strategies have been proposed and explored to enhance delamination resistance [37–40]. These strategies can be broadly categorized into two main approaches, i.e., chemical modifications of the matrix or matrix-fiber interfaces [41–43], and physical changes in the laminated composite architectures [44–47]. It is worth noting that the details of these approaches will be discussed in subsequent sections. Additionally, in this field, it is essential to highlight the role of the crack growth resistance curve (R-Curve) in studying the

evolution of delamination damage [48,49]. The R-Curve illustrates the variation in strain energy release rate (SERR), also known as interlaminar fracture toughness (ILFT), during the different stages of crack growth, providing valuable insights into interlaminar properties and resistance to delamination. Therefore, based on this note, the primary objective of many researchers has been to shift the behavior of the R-Curve from a linear trend to a rising, non-linear trend, thereby improving the overall delamination resistance of laminated composite materials.

In conclusion, generally, it can be succinctly stated that delamination in laminated composites is one of the most critical and performance-limiting damage mechanisms. Therefore, a clear understanding of this phenomenon, particularly through the use of the R-Curve, is crucial for developing effective strategies to mitigate it. Also, this understanding is essential for ensuring the reliability of laminated composite materials in sensitive and safety-critical applications. Therefore, this study takes a comprehensive and review-oriented approach to examine both the crack growth resistance in composite laminates under the shearing mode of loading (mode II, Fig. 1b) and the various strategies proposed to enhance delamination resistance. It should be noted that while extensive investigations have been conducted on delamination under opening-mode loading (mode I, Fig. 1a), a focused new review of mode II crack-growth resistance, which is considered one of the most relevant and practical loading modes in engineering applications [49], was found to be essential. Also, this need prompted the selection of the present research topic, particularly in light of recent advancements aimed at improving this property. To this end, the present study begins with a comprehensive overview of the R-Curve in polymeric laminated composite materials, including its significance and the experimental methods and data analysis techniques used for evaluation. It then provides an in-depth discussion of the mechanisms, conventional approaches, and emerging strategies designed to improve the R-Curve and enhance mode II crack growth resistance in these materials. Importantly, this review aims to provide both researchers and engineers with a broad and practical perspective by clarifying effective mechanisms and applicable solutions. This will help identify and adopt innovative and optimized approaches for achieving superior performance, durability, and reliability in polymeric laminated composite materials.

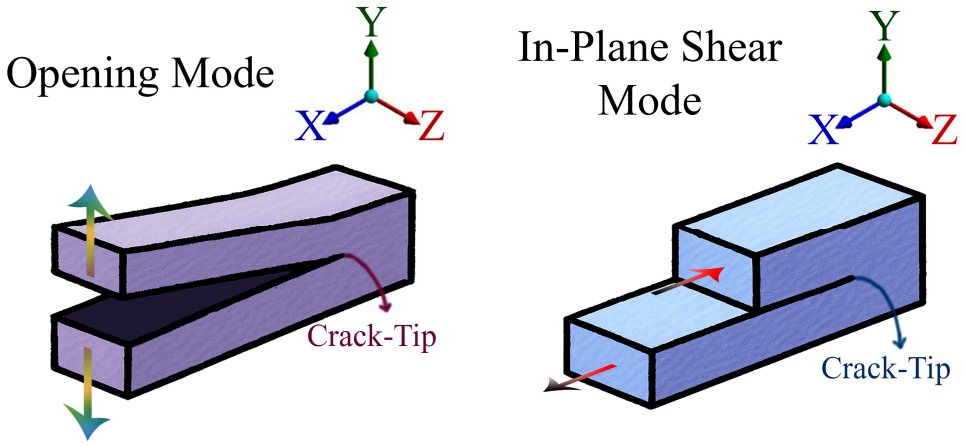

Figure 1: Schematic of interlaminar damage and crack growth under: (**a**) Mode I loading; (**b**) Mode II loading.

Therefore, it can be said that this review aims to answer three concrete questions:

- How do different interface designs (e.g., interlayers, yarn architectures) influence the shape and magnitude of the mode II crack growth resistance curve?

- Are current standard tests and data reduction methods, i.e., compliance calibration method (CCM) and the compliance-based beam method (CBBM), still reliable when toughening mechanisms create extensive bridging and large fracture process zones (FPZ)?
- Which toughening strategies are mature enough for structural application, and which remain limited to laboratory-scale coupons?

2 R-Curve and Its Importance

From fracture mechanics, when a crack exists in a material, the strain energy stored around the crack tip is released to create new crack surfaces and facilitate crack growth. To quantify this process, fracture mechanics introduces a parameter known as the strain energy release rate (SERR, G), which measures the energy released per unit increment of crack extension. In simple terms, if the energy provided by external loading exceeds the intrinsic resistance of the material at the crack interface, crack propagation will inevitably occur [50]. It is important to note that this parameter, for pure mode II loading, it is denoted as G_{II}. It should be noted that for certain types of materials, such as monolithic metals and some nanocomposites, this value tends to be constant. However, in many advanced materials, especially laminated composites, the resistance to crack propagation is not a constant value. In fact, as the crack propagates in these materials, the interactions at the crack tip and along the delamination interfaces may change, altering the crack growth resistance and SERR. In this field, to capture this behavior more accurately, the concept of the crack growth resistance curve is used. In other words, the R-Curve illustrates the relationship between crack extension (Δa) and the corresponding SERR required for further crack growth (See Fig. 2).

It should be noted that, as illustrated in Fig. 2, the crack-growth resistance of laminated composites can vary significantly after the initial crack initiation and during subsequent crack extension. This variation depends on the material characteristics and the active micromechanical or nanomechanical toughening mechanisms at the crack front and delamination surfaces in laminated composite materials [50–52]. For a more detailed explanation, in a rising R-Curve, the crack growth resistance increases with crack growth due to the activation of additional toughening mechanisms along the interfaces, ultimately reaching a saturation or steady-state level (see Fig. 2a,b). In addition, another type of R-Curve, i.e., a flat R-Curve, indicates that the resistance remains nearly constant after crack initiation, suggesting a lack of significant toughening mechanisms (refer to Fig. 2c). Conversely, a declining R-Curve, as demonstrated in Fig. 2d, shows that crack growth resistance decreases as the crack grows, which can result in sudden delamination, unstable crack propagation, and abrupt load drops in the affected structural component. It's also important to note that in some composite systems with complex architectures, a mixed response may occur.

Additionally, for a comprehensive understanding and practical application of the R-Curve in laminated composite materials, several key parameters are crucial (Fig. 2). For further explanation, one of the fundamental parameters is the ILFT value at crack initiation, denoted as $G_{IIC}^{ini.}$. This represents the energy required to initiate crack growth from the initial crack tip. It should be noted that in laminated composites, this value displays significant sensitivity to interfacial adhesion quality, fiber-matrix bonding, resin-rich regions, and microscopic imperfections [53,54]. Another important parameter is the propagation value of ILFT, represented as $G_{IIC}^{prop.}$. This parameter defines the critical energy level at which stable, steady-state crack growth occurs throughout the composite laminates, serving as an indicator of the structural safety margin and illustrating the extent to which the material can withstand a load before catastrophic delamination occurs. It is noteworthy that in systems exhibiting a rising R-Curve, $G_{IIC}^{prop.}$ consistently exceeds $G_{IIC}^{ini.}$ (as illustrated in Fig. 2a,b). In this field, it should be noted that a sustained rising R-Curve is usually linked to mechanisms that keep carrying load across the delamination surface behind the crack tip. Typical examples include fibre/yarn bridging (often stronger in woven composites due to transverse yarns), plastic deformation

of thermoplastic or porous interlayers, and crack deflection or pinning caused by interleaves. These effects expand the FPZ and increase the energy dissipated as the crack grows, which leads to a gradual rise in G_{II}.

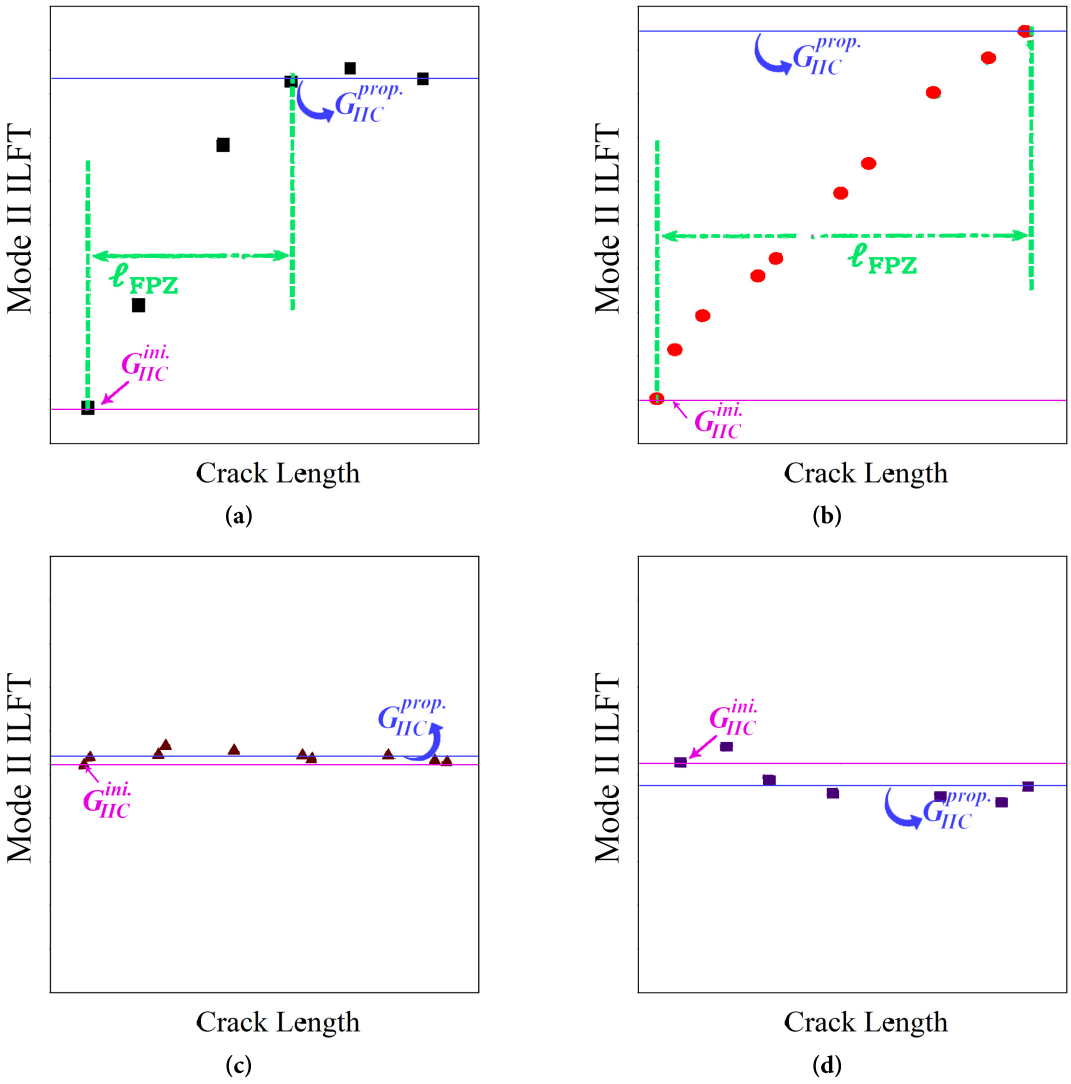

Figure 2: Schematic of common different types of R-curve: (**a**) rising-steady-state R-curve; (**b**) steadily rising R-curve; (**c**) flat R-curve; (**d**) declining R-curve.

Conversely, in instances where no toughening mechanisms are active, $G_{IIC}^{prop.}$ may equal (refer to Fig. 2c) or even fall below (refer to Fig. 2d) the initiation value. In fact, it can be said that if delamination growth is mainly controlled by matrix shear cracking with little bridging or limited load transfer at the interface, the FPZ stays relatively small, and GII usually reaches a steady plateau quickly.

Additionally, in this field, the fracture process zone length, l_{FPZ}, is another key parameter associated with the R-Curve. This length reflects the extent of the region ahead of the crack tip where micro-damage and toughening mechanisms operate. It is worth noting that l_{FPZ} is specifically defined as the difference in crack length between the $G_{IIC}^{ini.}$ and $G_{IIC}^{prop.}$ [55,56].

3 Achieving a Laminated Composite R-Curve under Mode II Loading

To obtain the R-Curve and evaluate the SERR in laminated composite specimens under mode II loading, where crack surfaces experience in-plane shear sliding, standardized experimental procedures, along with conventional data reduction methods, are commonly employed. Each of these approaches will be discussed in detail in the following sections.

3.1 Common Experimental Tests

One of the earliest experimental methodologies employed to investigate mode II ILFT in laminated composites was the short beam shear (SBS) test [57–59]. However, this method presented several inherent limitations, such as a relatively small span-to-thickness ratio and non-uniform stress distributions resulting from the applied load. These factors contradicted the assumptions of beam theory, which served as the foundation for most data reduction schemes [57,59]. In light of these challenges, subsequent refinements were introduced, and the classical framework of linear elastic fracture mechanics (LEFM) was utilized to ascertain the mode II ILFT/SERR in polymeric composite laminates. In this context, Barrett and Foschi [38], in 1977, employed the end-notched flexure (ENF) specimen to examine mode II ILFT in cracked wood beams. Subsequently, in 1982, Russel and Street [60] adopted the same ENF configuration to assess the critical ILFT/SERR of laminated composites.

It should be noted that, currently, the ENF specimen, in conjunction with the ASTM D7905 standard [61], is considered one of the most widely recognized experimental methods for determining mode II SERR of polymeric laminated composite materials. However, in addition to the primary methods, several other test configurations have been introduced over the years, although they have not gained widespread application like the ENF test specimens and ASTM D7905 standards. For example, in 1989 and 1990, Maikuma et al. [62,63] developed the center notch flexural (CNF) specimen to investigate mode II ILFT under both static and impact loading conditions.

3.2 Common Data Reduction Methods

As previously discussed, this review primarily focuses on the widely used ENF configuration for deriving R-Curves in composite laminates. Therefore, it particularly addresses the common data reduction methods associated with this specimen. In this context, it is essential to emphasize that mode II SERR/ILFT is typically determined in accordance with ASTM D7905 [61], utilizing the compliance calibration method (CCM). It should be noted that this method involves measuring the specimen's compliance at five different pre-crack lengths (i.e., 20, 25, 30, 35, and 40 mm). To achieve this, five-point compliance curves are created by conducting three-point bending tests at four non-critical crack lengths (20, 25, 35, and 40 mm). It is worth noting that, during these tests, the applied load is half of the fracture load. Subsequently, a mode II fracture test is performed at a crack length of 30 mm (see Fig. 3).

The CCM data reduction method is based on the study results of Irwin and Kies [64], as shown in Eq. (1). It should be noted that in this equation, the parameters P, a, and B are defined as critical load at a specified crack length, interlaminar crack length, and ENF specimen width, respectively.

$$G = \frac{P^2}{2B}\frac{dC}{da} \tag{1}$$

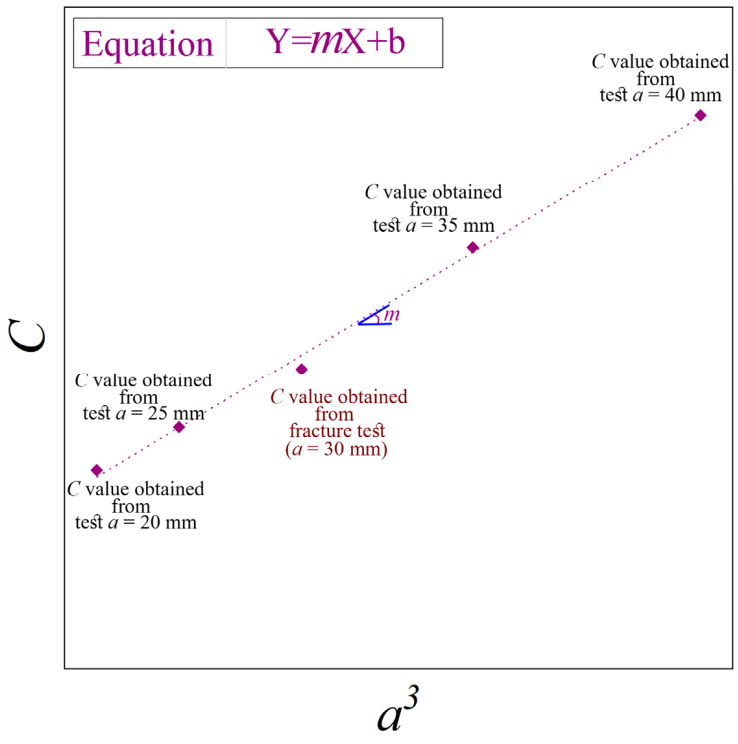

Figure 3: Calculation method of the *m* parameter.

However, the compliance parameter (C), based on Eq. (2), is experimentally calibrated using the initial compliance (C_0), the cube of the crack length (a^3), and the slope of the fitted line derived from the relationship between C and a^3 (m, as shown in Fig. 3).

$$C = C_0 + ma^3 \tag{2}$$

Finally, the mode II ILFT, as determined using the CCM (G_{IIc}^{CCM}), is calculated by combining Eqs. (1) and (2), as summarized in Eq. (3) [61].

$$G_{IIc}^{CCM} = \frac{3mP^2a^2}{2B} \tag{3}$$

It is important to note that accurately determining the mode II SERR/ILFT, based on CCM, requires simultaneous monitoring of load, load-point displacement, and visual crack length. This process can be experimentally challenging for specific materials and often results in significant errors. To overcome these limitations, de Moura et al. [65,66] proposed an alternative method based on beam theory, known as the compliance-based beam method (CBBM). This approach eliminates the need for direct crack length measurements by introducing the concept of an equivalent crack length (a_{eq}). Within this framework, the mode II ILFT, based on CBBM (G_{IIc}^{CBBM}), is directly derived from load-displacement data using Eq. (4), where h represents half the ENF specimen thickness [65,66].

$$G_{IIc}^{CBBM} = \frac{9P^2{a_{eq}}^2}{16B^2h^3E_f} \tag{4}$$

Also, the a_{eq} and equivalent flexural modulus (E_f) value in Eq. (4) are obtained from Eqs. (5) and (6), respectively, where L is the span length of the mode II ILFT test [65,66].

$$a_{eq} = \left[\frac{C_c}{C_{0c}}{a_0}^3 + \frac{2}{3}\left(\frac{C_c}{C_{0c}} - 1\right)\left(\frac{L^3}{2}\right)\right]^{\frac{1}{3}} \tag{5}$$

$$E_f = \frac{3{a_0}^3 + 2(\frac{L^3}{2})}{8Bh^3} \times (C_{0c})^{-1} \tag{6}$$

Additionally, the equivalent compliances associated with the initial compliance of the ENF specimen (C_{0C}) and the load-displacement curve (C_c) are calculated using Eqs. (7) and (8), respectively [65,66]. In these equations, the parameters C_0, C, and G_{13} represent the initial compliance, the equivalent compliance derived from the load-displacement data, and the out-of-plane shear modulus, respectively.

Notably, previous studies [65–67] suggest that the influence of G_{13} on the mode II SERR of laminated composites is minimal. Therefore, these parameters can be reasonably approximated using values reported in existing literature for similar materials, which negates the need for additional experimental measurements [65–67].

$$C_{0c} = C_0 - \frac{3(\frac{L}{2})}{10BhG_{13}} \tag{7}$$

$$C_C = C - \frac{3(\frac{L}{2})}{10BhG_{13}} \tag{8}$$

3.3 Limitation of Data Reduction Methods

The mode II ILFT test, based on ENF specimens, is commonly used for characterizing mode II fracture behavior. However, its reliability depends heavily on the accurate observation and measurement of delamination growth. In mode II loading, the delamination front is often hidden within the laminate and primarily propagates through interfacial sliding. This makes direct measurement of the crack length particularly challenging. Additionally, factors such as frictional sliding and local stick-slip behavior along the interface can complicate this process. Furthermore, the crack front may lose its uniformity or even branch, especially in laminates with toughened interfaces, such as those that include interleaves, through-thickness reinforcements (like Z-pins), or highly textured interfacial structures. When considered together, these phenomena create uncertainty in accurately determining the effective crack length and, more importantly, in identifying the true onset of crack propagation. Since the evaluation of SERR directly relies on these measurements, any ambiguity in tracking the crack front or detecting the initiation of cracks can significantly impact the reported values. Also, it should also be noted that extensive bridging and long FPZs may challenge classical LEFM assumptions, particularly the small-scale process zone requirement and the notion of self-similar crack advance. As a result, reported SERR values can represent an apparent toughness that includes bridging contributions and may exhibit sensitivity to specimen geometry and the adopted data-reduction procedure. This observation motivates the careful reporting of both initiation and propagation values.

In this context, selecting the appropriate data-reduction methodology is crucial. The CCM, as outlined in ASTM D7905, relies on direct measurements of crack length. Therefore, CCM is generally effective for determining the SERR when the crack front is easily identifiable, the FPZ is relatively small, and bridging

effects are minimal. Under these conditions, the interpretation aligns well with classical LEFM assumptions. However, when the crack front is obscured, uneven, or accompanied by branching or sub-cracking, conditions often observed in highly toughened interfaces, the reliability of crack-length tracking diminishes. In these scenarios, CCM becomes more dependent on the operator, and its accuracy in determining initiation values may be compromised, which can affect the comparability of results across different studies.

In contrast, the CBBM addresses a significant experimental challenge by eliminating the need for direct measurements of crack length. Instead, it utilizes an equivalent crack length that is inferred from the measured compliance. This feature makes CBBM particularly beneficial for systems where the physical crack tip is hard to observe or where crack-front irregularities are anticipated. Additionally, because it does not depend on visual tracking, CBBM reduces operator variability and is often regarded as a convenient method for constructing R-curves and assessing crack propagation.

3.4 Comparing the CCM and CBBM Data Reduction Methods

In summary, both the CCM and the CBBM have unique advantages and limitations. CCM is aligned with ASTM practices and is particularly effective for determining the SERR when the crack front is visible and bridging effects are minimal. However, its reliability decreases in scenarios involving hidden or branching crack fronts, and the results can be more dependent on the operator's skill.

On the other hand, CBBM removes the need for direct measurement of crack length, making it advantageous for analyzing propagation and evaluating R-curves. Nevertheless, in cases with significant bridging or long process zones, CBBM may produce higher apparent values of SERR because the compliance loss accounts for both crack advancement and the effects of bridging and the process zone.

Therefore, the choice between these methods should be based on the specific fracture mechanisms and interfacial architecture of the laminate being studied, as well as the intended focus on initiation vs. propagation behavior.

4 Mechanisms and Enhancement Factors

Up to this point, an overview was provided of laminated composites, delamination damage, the concept and importance of the R-Curve in delamination damage, and common standard experimental and data reduction methods used to characterize the R-Curve. Now, in this section, the main focus shifts to the parameters that govern the R-Curve in laminated composite materials subjected to mode II loading. In fact, this section explores explicitly the mechanisms that modify this curve, as well as proposed strategies to enhance it. To this end, the key factors, mechanisms, and approaches that contribute to the formation of the R-Curve and improve this behaviour will be discussed in detail. It is essential to emphasize that, given the critical need to enhance resistance to delamination in laminated composites, this review will focus on methods that result in either a consistently rising R-Curve or a two-stage response, i.e., an initial rising trend followed by a steady-state growth trend.

In this context, numerous studies have proposed various strategies to achieve an upward trend in the R-Curve and improve its performance under mode II loading. The primary goal of these approaches is to increase interlaminar friction, which enhances interlaminar energy absorption and slows the sliding of delamination interfaces. Additionally, these strategies aim to improve interlaminar interaction, which strengthens bonding, facilitates more efficient stress transfer across interfaces, and reduces stress concentration at the crack tip. Also, they seek to activate toughening mechanisms that resist crack propagation, such as fiber breakage, fiber bridging, crack pinning, and crack arresting. Therefore, in the following sections, several practical and widely adopted strategies in this field will be discussed in detail.

4.1 Stitching and Z-Pinning

In other words, a major weakness of laminated composites is the lack of reinforcing elements in the thickness direction, which results in poor performance in out-of-plane applications. Therefore, through-thickness reinforcement of laminated composites is an effective strategy for reducing delamination damage, commonly known as Z-pinning or stitching [46,68]. This approach aims to enhance the interaction between layers and improve the interfacial bonding in delamination areas of laminated composites. As a result, it boosts both the out-of-plane mechanical properties and the resistance to interlaminar crack propagation in laminated composites [69]. It is worth noting that the diameter of Z-pins is crucial in determining the effectiveness of this technique. For instance, Che et al. [70] studied how different Z-pin diameters impacted performance by using two sizes of carbon pins. Their results showed that reducing the pin diameter to 0.1 mm led to a 176% increase in mode II ILFT, while also reducing stress concentrations at the delamination interfaces. Also, this change shifted the primary fracture mechanism from Z-pin pullout to shear fracture.

Finally, it can be said that the through-thickness reinforcements, such as stitching and Z-pinning, effectively enhance delamination resistance by creating mechanical bridges and facilitating load transfer across interfaces. However, these advantages come with certain drawbacks that limit their universal application. For instance, disturbances to in-plane fibers, such as fiber waviness and localized damage, can impair in-plane properties, particularly compressive performance. Additionally, the introduction of extra materials and resin-rich zones may lead to increased mass, while the processes of insertion and manufacturing raise complexity and costs [70,71].

4.2 Changing in Fabrication Parameters

Processing and fabrication parameters are other critical factors that influence delamination resistance under mode II loading, as well as the overall trend of the R-Curve in laminated composites. In these fields, key variables such as curing temperature, heating rate of the curing process, post-curing conditions, and curing pressure [72–75] play a crucial role in determining the ILFT and delamination behavior of the composite laminate. In fact, it can be stated that by optimizing the curing temperature or pressure, or by applying an appropriate post-curing cycle, it is possible to enhance resin flow, promote interlaminar interaction and entanglement, and ultimately improve ILFT and the behavior of the R-Curve. It should be noted that when the specified parameters exceed their optimal limits, it can lead to several challenges, such as fiber degradation, microcracking within the matrix, or thermal damage. These challenges can negatively impact both ILFT and in-plane mechanical performance. For example, Liu et al. [76] found that increasing the curing temperature of carbon fiber-reinforced polymer laminates up to an optimal limit improves mode II ILFT of these composite laminates. This enhancement occurs due to improved resin flowability and better interfacial bonding. However, if the curing temperature is raised beyond this optimal point, it can cause excessive fluidity of the resin. This increased fluidity can expedite the lay-up process and boost the chances of bubble entrapment and porosity formation, ultimately leading to early defects that jeopardize the mechanical properties of the polymeric laminated composites. Also, Li et al. [77] examined how different curing pressures affect interlaminar properties in laminated composites. They found that applying a moderate pressure significantly enhances interlaminar entanglement, which in turn improves mode II ILFT. However, using excessive curing pressure can lead to fiber distortion and interfacial damage, ultimately decreasing delamination resistance in these composite laminates.

In other words, when optimizing the cure for thermosets, several key parameters, including cure temperature, pressure, heating rate, and post-cure conditions, play a crucial role. These factors influence resin flow, void content, and the quality of interlaminar bonds, all of which directly affect mode II delamination behavior. Also, in the case of thermoplastic laminates, *in-situ* consolidation parameters significantly impact

the level of intimate contact, healing between plies, and void formation. In fact, these aspects are critical for determining mode II resistance.

In conclusion, it should be noted that because of these sensitivities, it is crucial to control processing parameters precisely. In fact, this necessitates carefully designed manufacturing schedules and extensive optimization through repeated testing, which can pose practical challenges for large-scale industrial implementation.

4.3 Specific Stacking Sequence and Wave Pattern

The stacking sequence and ply orientation are crucial factors that determine the delamination resistance and ILFT of laminated composites [44,45,78–82]. Gong et al. [83] investigated the effects of various stacking sequences and demonstrated that the fiber orientation at the delamination interface of laminated composites plays a significant role in influencing mode II ILFT and R-Curve behavior. In this context, it can be stated that when the fiber lay-up is arranged so that transverse yarn bundles are aligned against the crack front, mechanisms such as fiber bridging and fiber breakage become more effectively activated, thus enhancing resistance to delamination and ILFT [84–86]. For instance, Ozdil et al. [87] found that polymeric composite laminates with a $[\pm 45]_5$ lay-up demonstrated higher ILFT values compared to those with $[\pm 30]_5$ and unidirectional configurations. This enhancement stems from the transverse alignment of fiber bundles at the delamination interface, which fosters a more uniform stress distribution and enhances resistance to both crack initiation and propagation. Also, Salamat-Talab et al. [88] discovered that incorporating glass fibers with an 8-harness (8H) satin weave in a transverse orientation at the delamination interfaces led to a fully rising R-Curve and enhanced mode II ILFT by about 27% compared to woven glass fabrics positioned at the same interface. However, when the same type of fiber (8H) was used with a longitudinal fiber orientation, the limited number of transverse yarn bundles resulted in moderate toughness improvement and failed to maintain a fully rising R-Curve due to the lack of continuous toughening mechanisms along the entire crack propagation path. Additionally, in another study, Ogasawara et al. [85] examined three different stacking sequences based on the orientation of yarn bundles in a 5H satin weave fiber at the delamination interface. Their findings indicated that when the majority of yarn bundles in the 5H satin weave fiber were oriented transversely, the ILFT was significantly enhanced, due to increased interaction between the fibers and matrix, as well as the activation of fiber bridging and fiber fracture mechanisms during the delamination process. It should be noted that in addition to the stacking sequence and yarn bundle orientation, factors such as the type of warp-weft pattern also affect delamination resistance [84,89–93].

4.4 Functionalization or Fiber Treatment

One of the key factors that enhances mode II delamination resistance in laminated composites is the surface functionalization or treatment of reinforcing fibers. These methods aim to improve the interlocking and interaction between fibers and the matrix, leading to stronger adhesion between the fibers and resin during crack propagation. As a result, more interlaminar energy can be absorbed through mechanisms like fiber bridging, fiber pull-out, and fiber breakage. This not only delays crack growth but also promotes a rising R-Curve and a more progressive fracture response [94–96]. For example, Qian et al. [97] demonstrated that applying oxygen plasma treatment for secondary layer functionalization significantly enhanced fiber-matrix adhesion, resulting in a 34% increase in mode II ILFT for glass/epoxy laminates. In fact, this improvement was primarily due to better interfacial bonding and the activation of energy-dissipating mechanisms, such as fiber bridging. Also, Zhao et al. [98] found that surface treatment of reinforcing fibers resulted in increases in mode II ILFT of laminated composites. These enhancements were linked to the formation of new functional

groups on the fiber surfaces, which improved fiber-matrix interfacial adhesion and encouraged mechanisms that resist cracks, thereby enhancing delamination resistance in the treated composites.

It is important to note that the physical parameters used during these treatments can significantly affect various mechanical properties of the polymeric composite laminates. In fact, if the processing parameters are not set correctly, they may damage the fiber surfaces, leading to a reduction in both interlaminar and in-plane properties, as well as an increase in fabrication costs [99–101].

4.5 Interleaving

In recent years, using interlayers in polymeric laminated composites has garnered significant attention as an effective method to improve ILFT or R-Curve behavior and reduce the risk of delamination in these materials. In fact, placing an interlayer at the fiber-matrix interfaces in laminated composites helps alleviate stress concentrations and interfacial discontinuities, ultimately improving the out-of-plane performance of these materials. Additionally, a key benefit of this approach is that while the out-of-plane behavior is greatly enhanced, the in-plane mechanical properties of the laminates are either maintained or may even be slightly improved [102–105].

When utilizing an interlayer as a secondary component between adjacent layers in laminated composites, it is crucial to have a thorough understanding of the primary damage modes and loading conditions. This knowledge allows for the design of an optimized interlayer that is specifically tailored to address the typical failure mechanisms in a given application, thereby ensuring enhanced delamination resistance and improved mechanical performance. For instance, for a mode II loading condition, an ideal interlayer should not only create a secondary bonding mechanism between the fibers and the resin but also improve interfacial friction. Additionally, it should activate interlaminar energy-absorbing mechanisms, such as fiber bridging and other processes that help arrest cracks. Accordingly, the choice of interlayer material system, along with its fabrication method and geometric configuration, is critically important.

Interlayers can be broadly classified based on their composition and structural characteristics into three categories: simple (single-component), hybrid (multi-component), and advanced or specific interlayers. Therefore, the following sections will discuss some of the most effective and widely studied interlayer configurations reported in recent literature.

4.5.1 Simple Interlayer

One category of interlayers consists of single-component materials, which typically include nanofibers or nano- and micro-scale particles. The main purpose of using these interlayers is to improve the interaction between adjacent layers in laminated composites and activate interlaminar mechanisms that resist cracking. For instance, nanofibrous interlayers can promote nanofiber bridging, while incorporating nano and micro particles into the structure can facilitate crack pinning [106].

In this field, it is noteworthy that a combination of structural and processing factors influences the efficiency of these interlayers in improving mode II ILFT. These include thickness [107–109], surface area density [110], the number of interlayer sheets [111], and the inherent properties of the materials used [106]. By optimizing these factors, it is possible to achieve a balance between interfacial adhesion, resin infiltration, and structural integrity. This optimization ultimately leads to a significant enhancement in the Mode II ILFT of laminated composites. For instance, Kheirkhah Barzoki et al. [107] demonstrated that using an electrospun polyvinyl Butyral (PVB) interlayer with an optimal thickness of 0.025 mm significantly enhanced mode II ILFT and resulted in an increasing R-Curve behavior in glass fiber reinforced composites. This improvement was attributed to adequate interfacial bonding and the activation of energy-absorbing mechanisms. In

contrast, increasing the interlayer thickness had a negative impact due to disrupted resin flow throughout the laminate. Similarly, Salimi-Mofrad et al. [108] reported that electrospun polyamide (PA) interlayers with a thickness of 0.11 mm resulted in an 84% increase in mode II ILFT. In another study, Bahmani et al. [110] explored the use of nonwoven polypropylene (PP) interlayers within glass/epoxy laminated composites. They discovered that incorporating an interlayer with a surface weight of 60% increased mode II ILFT by 56%. However, further increasing the areal density resulted in reduced toughness. This decline was attributed to hindered resin flow and inadequate interfacial contact.

Also, in the context of nano/micro fillers used as interlayers, Li and Li [111] reported that the incorporation of carbon nanotubes (CNTs) interlayers progressively improved mode II ILFT, achieving enhancements of up to 100% under optimal configurations. Shan et al. [112] demonstrated that applying CNTs interlayers onto carbon/epoxy composite laminates could increase ILFT by approximately 11% under optimized conditions. This enhancement was mainly attributed to the activation of mechanisms such as crack pinning and crack deflection. However, an excessive amount of CNTs disrupted interfacial bonding and adversely affected the interlaminar properties.

Finally, based on the aforementioned studies, it can be concluded that nanofibers primarily enhance mode II ILFT by introducing physical barriers that promote crack pinning and nanofiber bridging. However, the efficacy of these interlayers is fundamentally governed by a strict geometric trade-off regarding resin infiltration (which dictates interlaminar adhesion) and the mechanisms resisting crack propagation. For instance, as evidenced by the previously discussed studies, while optimizing the thickness and areal density of the interlayers yields significant improvements in crack growth resistance, exceeding the critical thresholds of these parameters inevitably disrupts resin flowability between the layers. This disruption weakens interlaminar contact and can even lead to a reduction in mode II ILFT. Similarly, while the incorporation of nanoparticles and the use of nanoparticle-based interlayers can enhance mode II ILFT under conditions of ideal dispersion, an excessive concentration of these materials rapidly makes the interface brittle, diminishes resin flowability, disrupts bonding, and intensifies stress concentration at the delamination interface, ultimately decreasing crack growth resistance

4.5.2 Hybrid Interlayer

As previously mentioned, single-component interlayers typically cannot activate all possible toughening mechanisms at the same time, which limits their effectiveness in preventing crack propagation. As a result, hybrid interlayers have gained significant attention in recent years. In fact, these interlayers offer combined material properties and can create multiscale interactions within the laminated composite structure. In this regard, Liu et al. [113] investigated a porous poly(ether sulfone) (PES)/CNTs hybrid interlayer and found that incorporating this interlayer significantly improved the mode II ILFT of carbon/epoxy laminated composites. Also, Zhang et al. [114] used an electrospun hybrid interlayer made from PES, polyphthalamide ether nylon ketone (PPENK), and polyphthalamide ether ketone (PBPESK) hybridized with zinc oxide nanowires. They reported that optimizing the nanowire deposition enhanced the ILFT. Also, in a related study, Kazemi et al. [106] developed an innovative green composite nanoparticle system that features a silica core and a magnesium hydroxide shell. They incorporated 0.75 wt% of these nanoparticles into electrospun poly(vinyl alcohol) (PVA) nanofibers [106]. Their findings demonstrated a 122% increase in mode II ILFT, along with a fully ascending R-Curve in glass/epoxy composite laminates. In this regard, it should be noted that this significant resistance to crack propagation was attributed to enhanced interfacial adhesion and secondary bonding between the PVA nanofibers and the epoxy matrix. Additionally, factors such as the breakage of the nanofibers, nanofiber bridging, and crack pinning (facilitated by the green composite nanoparticles) contributed to this improved performance.

4.5.3 Advanced and Specific Interlayer

In addition to all the aforementioned interlayers, recently, new interlayer architectures and innovative fabrication methods have gained attention, particularly three-dimensional (3D)-printed and mesh-structured interlayers. It should be noted that these approaches offer significant environmental and economic benefits [115,116]. In this context, Beylergil and Duman [115] used a 3D-printed PA interlayer designed with a mesh-like structure, resulting in an impressive 81% improvement in mode II ILFT for carbon/epoxy laminated composites. Similarly, Salamat-Talab and Kazemi [116] investigated how the type of filament material (wood/Poly(lactic Acid) (PLA) and PVA) and the thickness of 3D-printed interlayers, with cellular structure, affect the R-Curve behavior and mode II ILFT of polymeric laminated composites. They found that increasing the 3D-printed interlayer thickness up to 0.4 mm resulted in an improvement in mode II ILFT by as much as 70%, leading to a fully rising R-Curve (particularly with PVA interlayer). Generally, it can be stated that the resin-rich areas within these 3D-printed interlayers developed stronger adhesion, while the reinforcing filaments served as microstructural barriers, activating mechanisms for crack pinning and arresting during the propagation of mode II delamination. Furthermore, their results showed that the 3D-printed wood/PLA interlayers were effective in resisting crack growth, even at higher loading rates of up to 50 mm/min [53]. Also, Zhang et al. [117] reported a 69% increase in mode II ILFT for glass fiber reinforced polymer composites that included a mesh-like PA interlayer. They attributed this improvement to several energy-absorbing interlaminar mechanisms, such as PA fiber bridging, plastic deformation, fiber fracture, and the interlayer's capability to induce controlled crack deflection and guidance.

In this section, we can conclude that interlayers, specifically simple, hybrid, and architectured types, are among the most promising methods for enhancing mode II delamination resistance. This is due to their ability to be specifically tailored to selected interfaces without the need to modify the overall resin system. However, several important questions remain regarding their structural adoption, particularly concerning durability, manufacturability, and scalability.

4.6 Using Particle-Reinforced in Matrix

The incorporation of reinforcements, particularly micro- and nano-fillers, into the matrix of laminated composites is a widely adopted method for enhancing their thermal, electrical, chemical, and mechanical properties, including resistance to interlaminar delamination [17,118]. In this section, it is important to highlight the distinction between matrix modification and local interface-engineering approaches. Matrix modification involves altering the resin throughout the entire laminate, such as by adding nanoparticles or fillers. This can impact viscosity, manufacturing conditions, cost, qualification requirements, and potentially the in-plane properties of the laminate. On the other hand, local interface design focuses on enhancing toughness at specific interfaces that are prone to delamination, without altering the overall resin system of the laminate.

In using particle-reinforced in matrix field, since the early 1990s, nanomaterials such as CNTs and graphene have emerged as innovative additives [119,120]. These materials have demonstrated their effectiveness in improving delamination resistance of polymeric composite laminates, under various loading conditions, and in facilitating the formation of R-Curves [121–123]. In this context, Akhavan-Safar et al. [124] demonstrated that incorporating micro-cork particles, as fillers, within the matrix phase of glass/epoxy laminates can significantly enhance the mode II ILFT. Liu et al. [125] explored the synergistic effects of hybrid multi-walled CNTs (MWCNTs) and graphene oxide, as nanofillers, on mode II ILFT and reported remarkable improvements of up to 215% compared to reference specimens. It should be mentioned that these enhancements were attributed to the activation of reinforcing mechanisms such as improved fiber-matrix

interfacial interactions and crack arresting. Similarly, Soyugüzel et al. [126] found that adding nitrogen-doped reduced graphene oxide particles to carbon/epoxy laminated composites activated crack-pinning mechanisms at the delamination interface, resulting in a 45% increase in mode II ILFT.

Generally, the studies demonstrate that the improvements in delamination resistance and crack growth behavior due to matrix reinforcements can be primarily attributed to several factors:

- Stronger interlaminar bonding, resulting from the infiltration of nanoparticles into both the matrix and the reinforcing fibers.
- Increased interfacial friction at the interfaces of the laminated composite layers, which is enhanced by the presence of nanoparticles.
- Activation of interlaminar energy-dissipating mechanisms, including crack bridging and crack arresting.
- Redistribution of stress, which helps alleviate stress concentration at the crack tip.

Nevertheless, this approach has its limitations and potential drawbacks. In other words, some nanofillers or excessive filler loading can increase the hydrophilicity of the matrix, reduce the operational temperature range, elevate moisture uptake, and raise resin viscosity, potentially hindering the uniform dispersion of particles. As a result, particle accumulation within the resin can create zones of stress concentration, negatively impacting crack growth resistance and decreasing both interlaminar and in-plane mechanical properties of laminated composites [127,128]. For example, Srivastava et al. [129] demonstrated that adding 3 wt.% of multi-walled CNTs or graphene enhanced mode II ILFT in carbon/epoxy composites by 29% and 53%, respectively. In contrast, the addition of 3 wt.% carbon black, due to its high aggregation and poor dispersion, disrupted interlaminar bonding and resin flow, leading to a 43% decrease in mode II ILFT.

In conclusion, while the addition of micro- and nanofillers typically increases ILFT and encourages the formation of favorable R-Curves, achieving uniform dispersion of particles within the matrix is essential, as this uniformity allows for the full realization of benefits from mechanisms such as crack arresting, fiber bridging, and stress redistribution. In fact, these factors collectively contribute to reliable improvements in interlaminar delamination resistance and the development of R-Curves in polymeric laminated composite materials.

Furthermore, it is worth noting that the incorporation of high-surface-area fillers fundamentally alters the rheology of the matrix. This creates significant challenges in ensuring uniform particle dispersion, and often severely limits the use of infusion-based manufacturing processes due to premature resin gelation and the creation of localized stress concentrations in areas where particles agglomerate.

4.7 A Comparison of the Most Common Methods

While the strategies discussed earlier improve mode II ILFT and R Curve behavior, choosing a specific method for practical use requires carefully considering the trade-offs between mechanical performance, technological readiness, and industrial feasibility. For instance, macroscale techniques like stitching and Z pinning, though proven to enhance ILFT, often lead to a noticeable reduction in in-plane properties and increased manufacturing complexity, both of which create significant operational challenges.

Also, matrix modification through the incorporation of micro and nanoscale fillers offers a pathway toward achieving multifunctional properties throughout the composite laminates. Nevertheless, this approach substantially alters the rheological characteristics of the resin bulk, frequently leading to increased viscosity, a higher likelihood of particle agglomeration, the formation of stress concentration, and ultimately the initiation of microcracks in these laminated composite structures. Collectively, these factors may deteriorate the mechanical performance of the final structure and thus constitute important barriers to

the broader im-plementation of this strategy. Similarly, approaches based on interleaving directly target the delamina-tion prone interfaces while preserving in plane performance. Consequently, these approaches can substantially improve resistance to crack propagation and mode II ILFT. However, a notable difference persists in how these methods are technologically advanced, especially when considering more complex versions. Indeed, despite the impressive performance of these technologies in laboratory scale, their implementation in industrial production is still impeded by challenges associated with scalability and long-term reliability

Finally, it should be noted that, in addition to the aspects outlined above, a more comprehensive understanding and systematic comparison of these strategies is facilitated in the following section. Table 1 provides a concise overview of the mechanisms, advantages, limitations and trade-offs, industrial maturity, and the most suitable application domains for the crack-propagation resistance enhancement approaches discussed.

Table 1: Comparative assessment of toughening strategies in delamination-prone laminated composites: primary mechanisms, advantages, trade-offs, industrial maturity, and optimal application domains.

Toughening Strategy	Primary Crack Growth Resistance Mechanisms	Advantages	Trade-Offs	Industrial Maturity	Best Applicability
Through-Thickness Reinforcement (Z-Pinning/ Stitching)	Load transfer across interfaces; Mechanical bridging	Enhance out-of-plane properties; Improve interfacial bonding; Robust damage tolerance	Disturbs in-plane fibers; Reduces compressive strength; Reduces in-plane properties; Adds mass and manufacturing complexity	High (Industrial scale)	Aerospace joints; Highly effective for thick laminates
Fabrication parameters Optimization	Promotes interlaminar entanglement; Optimized resin flow	No added weight; No secondary materials required	Narrow processing windows; Risk of voids; Thermal damage; Micro-cracking (if limits are exceeded)	High (Industrial standard)	Autoclave processing; General composite panel manufacturing
Stacking Sequence and Wave Pattern	Transverse fiber bridging; Fiber breakage; Uniform stress distribution	Zero-cost implementation; Driven entirely by design	Constrained by global structural load requirements; Anisotropic response	High (Industrial standard)	Multi-directional laminates where lay-up flexibility is permitted
Fiber Functionalization or Fiber Treatment	Enhanced fiber-matrix adhesion; Fiber pull-out; Fiber bridging	Improves baseline fiber-resin compatibility at a micro-level	Incorrect parameters can damage fiber surfaces; Increases fabrication costs	Medium to High (Commercial sizing available)	Sizing applications during raw fiber manufacturing
Interleaving	Crack pinning; Crack deflection; Plastic deformation; Nanofiber pull-out; Nanofiber bridging	Enhance out-of-plane properties; Preserves in-plane properties; Can be localized to specific weak interfaces	High sensitivity to thickness; Unproven long-term fatigue durability	Low to Medium (Lab-scale to early commercial)	Prepreg systems; Specific interfaces highly prone to delamination

(Continued)

Table 1 (continued)

Toughening Strategy	Primary Crack Growth Resistance Mechanisms	Advantages	Trade-Offs	Industrial Maturity	Best Applicability
Particle-Reinforced Matrix	Global matrix bonding; Increased interfacial friction; Crack arresting; Stress redistribution	Multi-functional benefits (e.g., thermal, electrical); Independent of lay-up sequence	Drastically increases resin viscosity; High risk of particle agglomeration; Increases moisture uptake	Medium (Varies by filler type)	Liquid composite molding where uniform dispersion and viscosity can be controlled

Also, based on the previous mentions and Table 1, it can be stated that among the numerous strategies available, one of the most commonly used methods to enhance out-of-plane properties and increase delamination resistance in polymeric laminated composite materials, without significantly affecting in-plane performance, is the incorporation of secondary layers (i.e., interlayers) or local modifications at the delamination interface [102–104]. Consequently, to provide a comprehensive overview, Table 2 summarizes various interleaving and interfacial modification techniques documented in the literature, along with their respective effects on mode II ILFT of polymeric laminated composites. It is important to note that all reported improvements are expressed as percentage changes relative to the reference laminates that did not undergo interlayer and interfacial modifications.

Table 2: A thorough comparison of the effectiveness of common methods for enhancing the mode II ILFT of polymeric laminated composites, based on relevant research literature*, **.

Type of Strategies	Baseline Laminat	Compared to	R-Curve Behavior	Change in $G_{IIC}^{ini.}$ (%)	Change in $G_{IIC}^{prop.}$ (%)	[Ref.]
➢ **Changing the laminated composite layers: Using a specific fiber at delamination interfaces or a specific stacking sequence**						
Cotton fiber at delamination interfaces	Glass/Epoxy	Glass fiber	–	–	+212	[130]
Kenaf fibers at delamination interfaces	Glass/Epoxy	Glass fiber	–	–	+144	[130]
Transverse 5H fibre lay-up	Carbon/Epoxy	Unidirectional lay-up	Slight rising and then steady state	–	+55	[85]
Transverse 5H fibre	Glass/Epoxy	Plain weave fiber	Steadily rising	+112	+28	[88]
Longitudinal 5H fiber at delamination interfaces	Glass/Epoxy	Plain weave fiber	Rising and then steady state	+651	+16	[88]

(Continued)

Table 2 (continued)

Type of Strategies	Baseline Laminat	Compared to	R-Curve Behavior	Change in $G_{IIC}^{ini.}$ (%)	Change in $G_{IIC}^{prop.}$ (%)	[Ref.]
0°//60° lay-up	Glass/Epoxy	0°//0° lay-up	Rising and then steady state	–	+1	[131]
0°//15° lay-up	Glass/Epoxy	0°//0° lay-up	Flat plateau	−3	−2	[131]
➢ **Matrix Modification: Using Nano-/Micro-filler or particle in matrix phase**						
MWCNTs/graphene oxide nano-filler	Carbon/Epoxy	Without micro-filler	–	–	+215	[125]
MWCNTs/core-shell rubber nano-filler	Carbon/Epoxy	Without nano-filler	–	–	+80	[132]
CNTs nano-filler	Carbon/Epoxy	Without nano-filler	–	–	+63	[133]
Carbon nanofibers/silica/ short carbon fibers	Glass/Epoxy	Without nano-filler	–	–	+35	[134]
Micro-cork filler	Glass/Epoxy	Without nano-filler	Rising and then steady state	+127	+31	[124]
➢ **Interfaces Modification: Using an interlayer at delamination interfaces**						
3D network graphene	Glass/Epoxy	Without interlayer	–	–	+206	[135]
PVA nanofiber hybridized with nano-cork	Glass/Epoxy	Without interlayer	Steadily rising	+110	+201	[106]
Modified veils of PA-based nanofibrous	Carbon/Epoxy	Without interlayer	–	–	+134	[136]
Polyimide (PI) nanofibers	Carbon/ Polyimide	Without interlayer	–	–	+130	[137]
Hybrid film of epoxy and CNTs	Carbon/Epoxy	Without interlayer	–	–	+126	[138]

(Continued)

Table 2 (continued)

Type of Strategies	Baseline Laminat	Compared to	R-Curve Behavior	Change in $G_{IIC}^{ini.}$ (%)	Change in $G_{IIC}^{prop.}$ (%)	[Ref.]
PI/Polyvinyl pyrrolidone core–shell veils containing CNTs	Carbon/poly ether sulfone ketone	Without interlayer	–	–	+113	[139]
Wet veil of short-cut aramid fiber	Carbon/Epoxy	Without interlayer	–	–	+108	[140]
Bucky CNT paper	Carbon/Epoxy	Without interlayer	–	–	+104	[141]
Cellulose nanofibers hybridized with flax mat fibers	Carbon/Epoxy	Without interlayer	–	–	+100	[142]
PEK film	Carbon/Epoxy	Without interlayer	Steadily rising	+98	+91	[143]
Protein-surface-treated CNTs	Carbon/Epoxy	Without interlayer	–	–	+85	[144]
3D-printed of PA mesh	Carbon/Epoxy	Without interlayer	–	–	+81	[115]
3D-printed cellular structures of PVA filament	Glass/Epoxy	Without interlayer	Steadily rising	+57	+73	[116]
PVA nanofiber hybridized with green nanoparticles	Glass/Epoxy	Without interlayer	Steadily rising	+46	+72	[106]
Polyethylene terephthalate film	Carbon/Epoxy	Without interlayer	Steadily rising	+67	+70	[143]
PES film hybridized with graphene oxide	Carbon/Epoxy	Without interlayer	–	–	+70	[145]
Woven mesh polyamide	Glass/Epoxy	Without interlayer	–	–	+69	[117]

(Continued)

Table 2 (continued)

Type of Strategies	Baseline Laminat	Compared to	R-Curve Behavior	Change in $G_{IIC}^{ini.}$ (%)	Change in $G_{IIC}^{prop.}$ (%)	[Ref.]
CNTs grown on carbon fiber	Carbon/Epoxy	Without interlayer	–	–	+60	[146]
Flax mat fiber	Carbon/Epoxy	Without interlayer	–	–	+59	[142]
3D-printed cellular structures of wood/PLA filament	Glass/Epoxy	Without interlayer	Rising and then steady state	+83	+56	[116]
Spun-bonded PP	Glass/Epoxy	Without interlayer	–	–	+56	[110]
CNTs-decorated Poly-caprolactone nanofibers	Carbon/Epoxy	Without interlayer	–	–	+44	[147]
Polycaprolactone nanofibers hybridized with CNTs	Carbon/Epoxy	Without interlayer	–	–	+44	[147]
Oxygen plasma functionalized polycarbonates	Glass/Epoxy	Without interlayer	–	–	+42	[97]
PA nanofibers	Carbon/Epoxy	Without interlayer	–	–	+40	[148]
Sandwich structure, CNTs/PEK/CNTs	Carbon/Epoxy	Without interlayer	–	–	+38	[149]
Polyvinyl alcohol nanofiber	Glass/Epoxy	Without interlayer	Steadily rising	+17	+36	[150]
Thermoplastic polyurethane nanofibrous	Carbon/Epoxy	Without interlayer	–	–	+32	[151]
Short carbon fiber	Carbon/Epoxy	Without interlayer	–	–	+32	[152]
Sandwich structure, PEK/CNTs/PEK	Carbon/Epoxy	Without interlayer	–	–	+28	[149]

(Continued)

Table 2 (continued)

Type of Strategies	Baseline Laminat	Compared to	R-Curve Behavior	Change in $G_{IIC}^{ini.}$ (%)	Change in $G_{IIC}^{prop.}$ (%)	[Ref.]
PVA electrospun nanofiber	Glass/Epoxy	Without interlayer	Rising and then steady state	+50	+27	[106]
Polycaprolactone nanofibers	Glass/Epoxy	Without interlayer	Steadily rising	–	+24	[153]
Core-shell of graphene oxide-decorated polyurethane	Carbon/Epoxy	Without interlayer	–	–	+21	[154]
Spray coated CNTs	Carbon/Epoxy	Without interlayer	–	–	+19	[112]
Ultrafine epoxy fibers	Glass/Epoxy	Without interlayer	Slight rising and then steady state	–	+17	[155]
Polysulfone nanofibers	Carbon/Epoxy	Without interlayer	–	–	+17	[156]
PES nanofiber	Carbon/Epoxy	Without interlayer	–	–	+16	[157]
Carbon-Glass non-woven veils	Glass/Epoxy	Without interlayer	–	–	+13	[158]
PLA thin film	Carbon/Epoxy	Without interlayer	Steadily rising, (smooth)	–	+12	[159]
PLA thin film	Carbon/Epoxy	Without interlayer	Steadily rising, (smooth)	+1	+8	[159]
Polyether amide nanofibers hybridized with nanocellulose	Carbon/Epoxy	Without interlayer	–	+20	–	[160]

Note: *All of the data is sorted by the best results in any section within this table; **The symbol "–" indicates that the item was not presented by the reference study.

5 Conclusions, Limitations, and Outlook

5.1 Key Conclusions from the Current Literature

In recent years, polymeric laminated composites have been essential in high-performance structures. However, their reliability is significantly limited by weak interlaminar bonding. In fact, the lack of through-thickness reinforcement in laminated composite materials, along with the variability at the fiber-matrix interface, creates stress discontinuities that severely compromise performance in out-of-plane directions. This makes delamination a major and often undetected failure mode. Therefore, it is crucial to understand the mechanisms that govern interlaminar crack growth and interlaminar delamination failure. It is important to note that delamination behavior is highly dependent on the loading mode, and among these modes, mode II loading conditions hold particular significance, due to significant shear stresses encountered in practical applications. In this field, the review of related studies indicates that the primary goal of various strategies is to enhance mode II ILFT and delamination resistance in laminated composites by increasing the interaction and friction between layers in laminated composites. For instance, some traditional methods, such as stitching, Z-pinning, matrix toughening, and fiber surface functionalization or treatment, aim to improve the mode II ILFT of laminated composites. However, these approaches often come with trade-offs, including issues like stress concentrations, agglomeration effects, increased costs, environmental concerns, and potential degradation of in-plane properties. Therefore, a notable shift in perspective has emerged: rather than using some traditional methods, recent research is increasingly focusing on interface engineering. For example, more efficient alternatives have emerged in the field of composite materials, such as the modification of ply stacking sequences. This approach aims to introduce additional transverse yarns, which activate more bridging and crack-arresting mechanisms. Another effective strategy is the incorporation of interlayers, which improve interlaminar interaction, reduce stress discontinuities, and activate multiple toughening mechanisms. In fact, these methods can enhance out-of-plane performance without compromising, and in some cases even improving, the in-plane mechanical properties. It is worth mentioning that in the field of interleaving, recent research indicates that early single-component interlayers, although beneficial, are progressively being replaced by more complex hybrid or architectured interlayers. These advanced configurations can promote multiple toughening mechanisms simultaneously, such as increased interfacial friction, enhanced chemical bonding, and the formation of physical barriers to crack propagation. In conclusion, this approach represents a crucial pathway for developing high-performance composite materials that can resist hidden damages, such as delamination, while also extending their long-term structural durability in challenging service environments.

5.2 Limitations and Outlook

5.2.1 Limitations of Data Reduction

The mechanisms that enhance the apparent mode II ILFT, such as engineered interlayers, tailored stacking sequences, and interface-driven toughening, can also lead to non-classical fracture behavior. This means that in highly toughened systems, we may increasingly observe features like extended FPZs, strong fiber bridging, friction-dominated sliding, crack-front non-uniformity, and non-self-similar crack propagation. These characteristics fundamentally challenge the core assumptions of linear elastic fracture mechanics (LEFM), which include small-scale yielding and self-similar crack growth. As a result, standard characterization procedures that rely on the ENF method and beam-theory-based data reduction methods, such as ASTM D7905 using the CCM or CBBM, may not accurately represent the true fracture mechanics when large FPZs and bridging-dominated mechanisms are at play. In these situations, parameters like initiation and propagation value of ILFT can become sensitive to interpretation, dependent on geometry, and potentially non-transferable to structural design allowables.

5.2.2 Durability and Service Realism

Beyond the limitations of formulation, these interface-engineering strategies present several practical challenges. While results from laboratory-scale experiments show significant increases in delamination resistance and prolonged rising R-Curves, questions remain about their durability in service environments and long-term stability in aerospace or automotive structures. Therefore, future research should focus not only on enhancing toughness incrementally but also on establishing methodological rigor and scalability.

Also, most of the reported improvements have been demonstrated through quasi-static ENF testing. However, comprehensive validation under conditions such as shear fatigue, cyclic degradation of bridging mechanisms, environmental aging (particularly in hot and wet conditions), impact loading, and compression after impact is still limited. Since the contributions from friction and bridging may change with repeated loading and environmental exposure, their long-term stability has not yet been fully established.

5.2.3 Manufacturability and Large-Scale Implementation

While architected and hybrid interlayers enhance design possibilities, challenges remain in achieving consistent industrial-scale production. Key concerns include their integration with automated lay-up or out-of-autoclave processes, sensitivity to porosity and areas with excess resin, and ensuring quality assurance in thick or complex components. Conducting demonstrations beyond the laboratory scale is crucial to validate their robustness, reproducibility, and readiness for certification.

Finally, it should be noted that addressing these interconnected challenges will shape the next generation of laminated composites that can resist hidden delamination damage while maintaining reliable performance at real structural scales.

Acknowledgement: Not applicable.

Funding Statement: The authors received no specific funding for this study.

Author Contributions: The authors confirm contribution to the paper as follows: Conceptualization, Mazaher Salamat-Talab, Hossein Kazemi and Mehdi Safari; Data collection, Hossein Kazemi; Interpretation of results, Hossein Kazemi; Reviewing it critically for important intellectual content, Hossein Kazemi, Mazaher Salamat-Talab and Mehdi Safari; Writing—original draft preparation, Hossein Kazemi; Writing—review and editing, Mazaher Salamat-Talab, Hossein Kazemi and Mehdi Safari; Supervision, Mazaher Salamat-Talab and Mehdi Safari; Project administration, Mehdi Safari. All authors reviewed and approved the final version of the manuscript.

Availability of Data and Materials: The data that support the findings of this study are available from the Corresponding Author, Mazaher Salamat-Talab, upon reasonable request.

Ethics Approval: Not applicable.

Conflicts of Interest: The authors declare no conflicts of interest.

Nomenclature and Abbreviations

Latin characters

a	Delamination length, (mm)
a_0	Initial crack length, (mm)
a_{eq}	Equivalent crack length, (mm)
Δa	Crack extension length, (mm)
C	Compliance of ENF laminated composite specimens, (N/m)
C_C	Equivalent compliance of the ENF specimens at each state of delamination, (mm/N)

C_0	Initial compliance of the ENF laminated composite specimens, (mm/N)
C_{0C}	Equivalent initial compliance of the ENF laminated composite specimens, (mm/N)
E_f	Equivalent elastic modulus of ENF specimens, (GPa)
G	Strain energy release rate, (J/m^2)
G_C	Critical value of strain energy release rate, (J/m^2)
G_{II}	Mode II interlaminar strain energy release rate, (J/m^2)
G_{IIC}	Critical value of Mode II interlaminar strain energy release rate, (J/m^2)
$G_{IIc}^{ini.}$	Initiation mode II ILFT, (J/m^2)
$G_{IIc}^{prop.}$	Propagation mode II ILFT, (J/m^2)
G_{13}	Out-of-plane shear modulus of ENF specimens (GPa)
h	Half of the thickness of ENF laminated composite specimens, (mm)
L	Span length of the mode II ILFT test, (mm)
l_{FPZ}	Length of the fracture process zone, (mm)
P	Critical load at a specified crack length, (N)

Abbreviations

3D	Three-dimensional
ASTM	American Society for Testing Materials
CBBM	Compliance-Based Beam Method
CCM	Compliance calibration method
CF/Epoxy	Carbon-Fiber/Epoxy
CMCs	Ceramic matrix composites
CNF	Center notch flexural
CNTs	Carbon nanotubes
ENF	End-Notch Flexure
FPZ	Fracture Process Zone
GF/Epoxy	Glass-Fiber/Epoxy
ILFT	Inter-Laminar Fracture Toughness
LEFM	Linear elastic fracture mechanics
MMCs	Metal matrix composites
MWCNTs	Multi-Walled Carbon Nano-Tubes
PA	Polyamide
PBPESK	Polyphthalamide ether ketone
PES	Porous poly(ether sulfone)
PI	Polyimide
PLA	Poly(lactic Acid)
PMCs	Polymer matrix composites
PP	Polypropylene
PPENK	Polyphthalamide ether nylon ketone
PVA	Poly(vinyl alcohol)
PVB	Polyvinyl Butyral PVB
R-Curve	Crack growth resistance curve
SBS	Short beam shear
SERR	Strain energy release rate

References

1. Egbo MK. A fundamental review on composite materials and some of their applications in biomedical engineering. J King Saud Univ Eng Sci. 2021;33(8):557–68. doi:10.1016/j.jksues.2020.07.007.
2. Oladele IO, Omotosho TF, Adediran AA. Polymer-based composites: an indispensable material for present and future applications. Int J Polym Sci. 2020;2020(1):8834518. doi:10.1155/2020/8834518.

3. Khan F, Hossain N, Mim JJ, Rahman SM, Iqbal MJ, Billah M, et al. Advances of composite materials in automobile applications—a review. J Eng Res. 2025;13(2):1001–23. doi:10.1016/j.jer.2024.02.017.
4. Kangishwar S, Radhika N, Sheik AA, Chavali A, Hariharan S. A comprehensive review on polymer matrix composites: material selection, fabrication, and application. Polym Bull. 2023;80(1):47–87. doi:10.1007/s00289-022-04087-4.
5. Sajan S, Philip Selvaraj D. A review on polymer matrix composite materials and their applications. Mater Today Proc. 2021;47(2):5493–8. doi:10.1016/j.matpr.2021.08.034.
6. Mortensen A, Llorca J. Metal matrix composites. Annu Rev Mater Res. 2010;40(1):243–70. doi:10.1146/annurev-matsci-070909-104511.
7. Ralph B, Yuen HC, Lee WB. The processing of metal matrix composites—an overview. J Mater Process Technol. 1997;63(1–3):339–53. doi:10.1016/S0924-0136(96)02645-3.
8. Donald IW, McMillan PW. Ceramic-matrix composites. J Mater Sci. 1976;11(5):949–72. doi:10.1007/BF00542312.
9. Karadimas G, Salonitis K. Ceramic matrix composites for aero engine applications—a review. Appl Sci. 2023;13(5):3017. doi:10.3390/app13053017.
10. Hsissou R, Seghiri R, Benzekri Z, Hilali M, Rafik M, Elharfi A. Polymer composite materials: a comprehensive review. Compos Struct. 2021;262:113640. doi:10.1016/j.compstruct.2021.113640.
11. Yang G, Luo S, Lai T, Lai H, Luo B, Li Z, et al. A green and facile microvia filling method via printing and sintering of Cu-Ag core-shell nano-microparticles. Nanomater. 2022;12(7):1063. doi:10.3390/nano12071063.
12. Kocakaya Z. Green synthetic biomaterials: synthesis, characterization and antimicrobial properties of lichen-derived nanomaterials. Ceram Int. 2024;50(17):30712–22. doi:10.1016/j.ceramint.2024.05.371.
13. Padhan B, Patel R, Bhowmik P, Roy A, Das J, Yu Y, et al. Recent advancements in nanocomposites-based antibiofilm food packaging. J Polym Mater. 2025;42(2):411–33. doi:10.32604/jpm.2024.059156.
14. Kim S, Ahn Y, Song SH, Lee D. Tungsten nanoparticle anchoring on boron nitride nanosheet-based polymer nanocomposites for complex radiation shielding. Compos Sci Technol. 2022;221(2):109353. doi:10.1016/j.compscitech.2022.109353.
15. Sen M. Nanocomposite materials. In: Nanotechnology and the environment. London, UK: IntechOpen; 2020. doi:10.5772/intechopen.93047.
16. Ariyagounder J, Veerasamy S. Experimental investigation on the strength, durability and corrosion properties of concrete by partial replacement of cement with nano-SiO_2, nano-$CaCO_3$ and nano-$Ca(OH)_2$. Iran J Sci Technol Trans Civ Eng. 2022;46(1):201–22. doi:10.1007/s40996-021-00584-0.
17. Kazemi H, Salamat-Talab M, Ghanbari D. Enhancing mechanical and thermal properties of nanocomposites using novel silica/$Mg(OH)_2$ green composite nanoparticles. J Inorg Organomet Polym Mater. 2025;35(1):356–73. doi:10.1007/s10904-024-03299-7.
18. Lee DW, Yoo BR. Advanced silica/polymer composites: materials and applications. J Ind Eng Chem. 2016;38:1–12. doi:10.1016/j.jiec.2016.04.016.
19. Jing Q, Liu W, Pan Y, Silberschmidt VV, Li L, Dong ZL. Chemical functionalization of graphene oxide for improving mechanical and thermal properties of polyurethane composites. Mater Des. 2015;85:808–14. doi:10.1016/j.matdes.2015.07.101.
20. Gobi N, Vijayakumar D, Keles O, Erogbogbo F. Infusion of graphene quantum dots to create stronger, tougher, and brighter polymer composites. ACS Omega. 2017;2(8):4356–62. doi:10.1021/acsomega.6b00517.
21. Hao T, Wang Y, Liu Z, Li J, Shan L, Wang W, et al. Emerging applications of silica nanoparticles as multifunctional modifiers for high performance polyester composites. Nanomaterials. 2021;11(11):2810. doi:10.3390/nano11112810.
22. Kumar D, Gururaja S, Jawahir IS. Machinability and surface integrity of adhesively bonded Ti/CFRP/Ti hybrid composite laminates under dry and cryogenic conditions. J Manuf Process. 2020;58(1):1075–87. doi:10.1016/j.jmapro.2020.08.064.
23. Kumar R, Singh RK, Singh DP. Natural and waste hydrocarbon precursors for the synthesis of carbon based nanomaterials: graphene and CNTs. Renew Sustain Energy Rev. 2016;58:976–1006. doi:10.1016/j.rser.2015.12.120.

24. Mega M, Dolev O, Banks-Sills L. Fracture toughness resistance curves for a delamination in CFRP MD laminate composites, Part II: mixed-mode deformation. Theor Appl Fract Mech. 2024;133(11):104583. doi:10.1016/j.tafmec.2024.104583.
25. Al-Shamary AKJ, Abed ARN, Karakuzu R. A comparative study on ballistic impact behaviors of glass/epoxy composites. Mech Adv Mater Struct. 2024;31(30):13341–50. doi:10.1080/15376494.2023.2256003.
26. Seif A, Allah MMA, Megahed M, Saeed Almuflih A, Abd El-baky MA. Hybridization of thermoplastic/glass fiber reinforced epoxy composites for lightweight structures. Mech Adv Mater Struct. 2025;32(14):3272–87. doi:10.1080/15376494.2024.2391545.
27. Abrate S. Impact on laminated composite materials. Appl Mech Rev. 1991;44(4):155–90. doi:10.1115/1.3119500.
28. Sela N, Ishai O. Interlaminar fracture toughness and toughening of laminated composite materials: a review. Composites. 1989;20(5):423–35. doi:10.1016/0010-4361(89)90211-5.
29. Torabizadeh MA, Shokrieh MM. An experimental and numerical study of the dynamic response of composites under impact at low temperatures. Mech Adv Mater Struct. 2016;23(6):615–23. doi:10.1080/15376494.2015.1017677.
30. Farrokhabadi A, Madadi H, Naghdinasab M, Rafie A, Ahmad Taghizadeh S, Herráez M. Micromechanical investigation of cross-ply carbon composite laminates with glass microtubes using CZM and XFEM. Mech Adv Mater Struct. 2022;29(26):5624–36. doi:10.1080/15376494.2021.1961177.
31. Bouvet C, Serra J, Perez PG. Strain rate effect of mode II interlaminar fracture toughness on the impact response of a thermoplastic PEEK composite. Compos Part C Open Access. 2020;2:100031. doi:10.1016/j.jcomc.2020.100031.
32. Khan A, Kim HS. A brief overview of delamination localization in laminated composites. Multiscale Sci Eng. 2022;4(3):102–10. doi:10.1007/s42493-022-00085-w.
33. Huang T, Bobyr M. A review of delamination damage of composite materials. J Compos Sci. 2023;7(11):468. doi:10.3390/jcs7110468.
34. Riccio A. Delamination in the context of composite structural design. In: Delamination behaviour of composites. Amsterdam, The Netherlands: Elsevier; 2008. p. 28–64. doi:10.1533/9781845694821.1.28.
35. Morita H, Adachi T, Tateishi Y, Matsumot H. Characterization of impact damage resistance of CF/PEEK and CF/toughened epoxy laminates under low and high velocity impact tests. J Reinf Plast Compos. 1997;16(2):131–43. doi:10.1177/073168449701600203.
36. Pai Y, Dayananda Pai K, Vijaya Kini M. Effect of ageing conditions on the low velocity impact behavior and damage characteristics of aramid-basalt/epoxy hybrid interply composites. Eng Fail Anal. 2023;152:107492. doi:10.1016/j.engfailanal.2023.107492.
37. Sridharan S. Delamination behaviour of composites. Amsterdam, The Netherlands: Elsevier; 2008.
38. Barrett JD, Foschi RO. Mode II stress-intensity factors for cracked wood beams. Eng Fract Mech. 1977;9(2):371–8. doi:10.1016/0013-7944(77)90029-7.
39. Pinto MA, Chalivendra VB, Kim YK, Lewis AF. Effect of surface treatment and Z-axis reinforcement on the interlaminar fracture of jute/epoxy laminated composites. Eng Fract Mech. 2013;114(7):104–14. doi:10.1016/j.engfracmech.2013.10.015.
40. Wilk J. Applicability of mode II interlaminar fracture toughness testing methods for characterization of thermoplastic laminates with woven fabric reinforcements. Eng Fract Mech. 2019;216(4):106533. doi:10.1016/j.engfracmech.2019.106533.
41. Li Y, Peng Q, He X, Hu P, Wang C, Shang Y, et al. Synthesis and characterization of a new hierarchical reinforcement by chemically grafting graphene oxide onto carbon fibers. J Mater Chem. 2012;22(36):18748–52. doi:10.1039/c2jm32596a.
42. Xu Z, Huang Y, Min C, Chen L, Chen L. Effect of γ-ray radiation on the polyacrylonitrile based carbon fibers. Radiat Phys Chem. 2010;79(8):839–43. doi:10.1016/j.radphyschem.2010.03.002.
43. Zhou X, Wang Y, Xiao M, Liu J, Wen J, Shen H, et al. Bagasse fibers surface heat treatment and its effect on mechanical properties of starch/poly (vinyl alcohol) composites. J Polym Mater. 2025;42(3):795–810. doi:10.32604/jpm.2025.068200.

44. Navarro P, Aubry J, Pascal F, Marguet S, Ferrero JF, Dorival O. Influence of the stacking sequence and crack velocity on fracture toughness of woven composite laminates in mode I. Eng Fract Mech. 2014;131(8):340–8. doi:10.1016/j.engfracmech.2014.08.010.
45. Monticeli FM, Fuga FR, Arbelo MA, Donadon MV. The effect of fibre orientation on fatigue crack propagation in CFRP: finite fracture mechanics modelling for open-hole configuration. Eng Fail Anal. 2024;161:108278. doi:10.1016/j.engfailanal.2024.108278.
46. Mouritz AP, Leong KH, Herszberg I. A review of the effect of stitching on the in-plane mechanical properties of fibre-reinforced polymer composites. Compos Part A Appl Sci Manuf. 1997;28(12):979–91. doi:10.1016/S1359-835X(97)00057-2.
47. Mouritz AP. Review of z-pinned laminates and sandwich composites. Compos Part A Appl Sci Manuf. 2020;139:106128. doi:10.1016/j.compositesa.2020.106128.
48. Mai YW. Cohesive zone and crack-resistance (R)-curve of cementitious materials and their fibre-reinforced composites. Eng Fract Mech. 2002;69(2):219–34. doi:10.1016/S0013-7944(01)00086-8.
49. Carlsson LA, Gillespie JW. Chapter 4—mode-II interlaminar fracture of composites. In: Friedrich K, editor. Composite materials series. Amsterdam, The Netherlands: Elsevier; 1989. p. 113–57. doi:10.1016/B978-0-444-87286-9.50008-5.
50. Nairn JA. Analytical and numerical modeling of R curves for cracks with bridging zones. Int J Fract. 2009;155(2):167–81. doi:10.1007/s10704-009-9338-3.
51. Herráez M, González C, Lopes CS. A numerical framework to analyze fracture in composite materials: from R-curves to homogenized softening laws. Int J Solids Struct. 2018;134(8):216–28. doi:10.1016/j.ijsolstr.2017.10.031.
52. Raimondo A. Numerical investigation of the R-curve effect in delamination of composite materials using cohesive elements. Appl Sci. 2024;14(6):2535. doi:10.3390/app14062535.
53. Salamat-Talab M, Kazemi H, Akhavan-Safar A, da Silva LFM. Loading rate influence on delamination behavior of reinforced ENF specimens by additively manufactured interlayer. J Compos Sci. 2025;9(9):494. doi:10.3390/jcs9090494.
54. Salamat-Talab M, Kazemi H, Akhavan-Safar A, Malekinejad H, Carbas RJC, da Silva LFM. Effects of a novel three-dimensional-printed wood–polylactic acid interlayer on the mode II delamination of composites. J Compos Sci. 2024;8(12):489. doi:10.3390/jcs8120489.
55. Ozdil F, Carlsson LA, Li X. Characterization of mode II delamination growth in glass/epoxy composite cylinders. J Compos Mater. 2000;34(4):274–98. doi:10.1177/002199830003400402.
56. Ozdil F, Carlsson LA. Characterization of mode I delamination growth in glass/epoxy composite cylinders. J Compos Mater. 2000;34(5):398–419. doi:10.1177/002199830003400503.
57. Whitney JM. Elasticity analysis of orthotropic beams under concentrated loads. Compos Sci Technol. 1985;22(3):167–84. doi:10.1016/0266-3538(85)90031-4.
58. ASTM D2344. Standard test method for short-beam strength of polymer matrix composite materials and their laminates. West Conshohocken, PA, USA: ASTM International; 2022. 10 p.
59. Whitney JM, Browning CE. On short-beam shear tests for composite materials. Exp Mech. 1985;25(3):294–300. doi:10.1007/BF02325100.
60. Russel A, Street K. Factors affecting the interlaminar fracture energy of graphite epoxy laminates. In: Hayashi KK, Umekawa S, editors. Proceedings of the Fourth International Conference on Composite Materials. Tokyo, Japan: Japan Society for Composite Materials; 1982. p. 279–86.
61. ASTM D7905/D7905M-19e1. Standard test method for determination of the mode II interlaminar fracture toughness of unidirectional fiber-reinforced polymer matrix composites. West Conshohocken, PA, USA: ASTM International; 2019. doi:10.1520/D7905_D7905M-19E01.
62. Maikuma H, Gillespie JW JR, Wilkins DJ. Mode II interlaminar fracture of the center Notch flexural specimen under impact loading. J Compos Mater. 1990;24(2):124–49. doi:10.1177/002199839002400201.
63. Maikuma H, Gillespie JW JR, Whitney JM. Analysis and experimental characterization of the center Notch flexural test specimen for mode II interlaminar fracture. J Compos Mater. 1989;23(8):756–86. doi:10.1177/002199838902300801.

64. Irwin GR, Kies J. Critical energy rate analysis of fracture strength. Spie Milest Ser MS. 1997;137:136–41.
65. de Moura MFSF, Campilho RDSG, Gonçalves JPM. Pure mode II fracture characterization of composite bonded joints. Int J Solids Struct. 2009;46(6):1589–95. doi:10.1016/j.ijsolstr.2008.12.001.
66. de Moura MFSF, Silva MAL, de Morais AB, Morais JJL. Equivalent crack based mode II fracture characterization of wood. Eng Fract Mech. 2006;73(8):978–93. doi:10.1016/j.engfracmech.2006.01.004.
67. Yan X, Guo X, Gao Y, Lin Y, Zhang N, Zhao Q. Mode-II fracture toughness and crack propagation of pultruded carbon Fiber-Epoxy composites. Eng Fract Mech. 2023;279(1):109042. doi:10.1016/j.engfracmech.2022.109042.
68. Partridge IK, Cartié DDR. Delamination resistant laminates by Z-Fiber® pinning: part I manufacture and fracture performance. Compos Part A Appl Sci Manuf. 2005;36(1):55–64. doi:10.1016/j.compositesa.2004.06.029.
69. Jain LK, Dransfield KA, Mai YW. On the effects of stitching in CFRPs—II. Mode II delamination toughness. Compos Sci Technol. 1998;58(6):829–37. doi:10.1016/S0266-3538(97)00186-3.
70. Che Z, Li M, Wang S, Wang S, Gu Y, Zhang W. Mode II interlaminar fracture toughness enhancement of fine z-pin reinforced carbon fiber composite with low fraction of pins. Polym Compos. 2022;43(5):2992–3002. doi:10.1002/pc.26593.
71. Yan W, Liu HY, Mai YW. Mode II delamination toughness of z-pinned laminates. Compos Sci Technol. 2004;64(13–14):1937–45. doi:10.1016/j.compscitech.2004.02.008.
72. Cartié D, Davies P, Peleau M, Partridge IK. The influence of hydrostatic pressure on the interlaminar fracture toughness of carbon/epoxy composites. Compos Part B Eng. 2006;37(4–5):292–300. doi:10.1016/j.compositesb.2005.12.002.
73. Tang JM, Lee WI, Springer GS. Effects of cure pressure on resin flow, voids, and mechanical properties. J Compos Mater. 1987;21(5):421–40. doi:10.1177/002199838702100502.
74. Chen C, Nesbitt S, Reiner J, Vaziri R, Poursartip A, Fernlund G. Cure path dependency of static and dynamic mode II interlaminar fracture toughness of interlayer toughened composite laminates. Compos Sci Technol. 2020;200:108444. doi:10.1016/j.compscitech.2020.108444.
75. Sajith S, Arumugam V, Dhakal HN. Effects of curing pressure on mode II fracture toughness of uni-directional GFRP laminates. Polym Test. 2015;48(3):59–68. doi:10.1016/j.polymertesting.2015.09.011.
76. Liu X, Qian S, Ye Y, Xu Q, Li X. Effect of process parameters on mode-II interlaminar fracture toughness and fractographic features of automated fibre placement prepreg laminates. J Compos Mater. 2021;55(30):4489–501. doi:10.1177/00219983211041761.
77. Li N, Wang GD, Melly SK, Peng T, Li YC, Qi DZ, et al. Interlaminar properties of GFRP laminates toughened by CNTs buckypaper interlayer. Compos Struct. 2019;208:13–22. doi:10.1016/j.compstruct.2018.10.002.
78. Chai H. Interlaminar shear fracture of laminated composites. Int J Fract. 1990;43(2):117–31. doi:10.1007/BF00036181.
79. Polaha JJ, Davidson BD, Hudson RC, Pieracci A. Effects of mode ratio, ply orientation and precracking on the delamination toughness of a laminated composite. J Reinf Plast Compos. 1996;15(2):141–73. doi:10.1177/073168449601500202.
80. Davidson BD, Krüger R, König M. Effect of stacking sequence on energy release rate distributions in multidirectional dcb and enf specimens. Eng Fract Mech. 1996;55(4):557–69. doi:10.1016/S0013-7944(96)00037-9.
81. Blanco N, Trias D, Pinho ST, Robinson P. Intralaminar fracture toughness characterisation of woven composite laminates. Part II: experimental characterisation. Eng Fract Mech. 2014;131:361–70. doi:10.1016/j.engfracmech.2014.08.011.
82. Zhou Y, Cao Y, Cao J, Zhang C, Li J, Wang Z. Fracture toughness and fiber bridging mechanism for mode-I interlaminar failure of spread-tow woven composites. Eng Fract Mech. 2024;298:109957. doi:10.1016/j.engfracmech.2024.109957.
83. Gong Y, Tao J, Chen X, Zhao J, Hu N. A semi-analytical method for determining mode-II fracture toughness and bridging law of composite laminates. Eng Fract Mech. 2022;265(16):108371. doi:10.1016/j.engfracmech.2022.108371.
84. Suppakul P, Bandyopadhyay S. The effect of weave pattern on the mode-I interlaminar fracture energy of E-glass/vinyl ester composites. Compos Sci Technol. 2002;62(5):709–17. doi:10.1016/S0266-3538(01)00220-2.

85. Ogasawara T, Yoshimura A, Ishikawa T, Takahashi R, Sasakib N, Ogawa T. Interlaminar fracture toughness of 5 harness satin woven fabric carbon fiber/epoxy composites. Adv Compos Mater. 2012;21(1):45–56. doi:10.1163/156855112X626219.
86. Alif N, Carlsson LA, Boogh L. The effect of weave pattern and crack propagation direction on mode I delamination resistance of woven glass and carbon composites. Compos Part B Eng. 1998;29(5):603–11. doi:10.1016/S1359-8368(98)00014-6.
87. Ozdil F, Carlsson LA, Davies P. Beam analysis of angle-ply laminate end-notched flexure specimens. Compos Sci Technol. 1998;58(12):1929–38. doi:10.1016/S0266-3538(98)00018-9.
88. Salamat-Talab M, Kazemi H, Mahdavi M. Influence of yarn bundle orientation and areal density on the interlaminar fracture toughness of ENF composites. Eng Fract Mech. 2025;315(2):110806. doi:10.1016/j.engfracmech.2025.110806.
89. Johnson WS, Masters JE, Wilson DW, Martin RH. Delamination characterization of woven glass/polyester composites. J Compos Technol Res. 1997;19(1):20. doi:10.1520/ctr10010j.
90. Ebeling T, Hiltner A, Baer E, Fraser IM, Orton ML. Delamination failure of a single yarn glass fiber composite. J Compos Mater. 1997;31(13):1302–17. doi:10.1177/002199839703101303.
91. Ebeling T, Hiltner A, Baer E, Fraser IM, Orton ML. Delamination failure of a woven glass fiber composite. J Compos Mater. 1997;31(13):1318–33. doi:10.1177/002199839703101304.
92. Funk JG, Deaton JW. The interlaminar fracture toughness of woven graphite/epoxy composites. Washington, DC, USA: NASA; 1989. 29 p. Report No.: NASA-TP-2950.
93. Reifsnider KL, Sendeckyj GP, Wang SS, Feng W, Johnson WS, Stinchcomb WW, et al. The effects of radiation on the interlaminar fracture toughness of a graphite/epoxy composite. J Compos Technol Res. 1986;8(3):92. doi:10.1520/ctr10328j.
94. Koohestani B, Darban AK, Mokhtari P, Yilmaz E, Darezereshki E. Comparison of different natural fiber treatments: a literature review. Int J Environ Sci Technol. 2019;16(1):629–42. doi:10.1007/s13762-018-1890-9.
95. Kehrer M, Rottensteiner A, Hartl W, Duchoslav J, Thomas S, Stifter D. Cold atmospheric pressure plasma treatment for adhesion improvement on polypropylene surfaces. Surf Coat Technol. 2020;403(1):126389. doi:10.1016/j.surfcoat.2020.126389.
96. Zhao H, Gao Z, Zhai D, Zhao G. Enhanced mechanical property of continuous carbon fiber/polyamide thermoplastic composites by combinational treatments of carbon fiber fabric. Compos Commun. 2023;38:101508. doi:10.1016/j.coco.2023.101508.
97. Qian X, Kravchenko OG, Pedrazzoli D, Manas-Zloczower I. Effect of polycarbonate film surface morphology and oxygen plasma treatment on mode I and II fracture toughness of interleaved composite laminates. Compos Part A Appl Sci Manuf. 2018;105(9):138–49. doi:10.1016/j.compositesa.2017.11.016.
98. Zhao Y, Fang C, Jia L, Shi B, Chen Z, Zhang X, et al. Influence of Oxygen/Argon/Nitrogen multi-component plasma modification on interlayer toughening of UHMWPE fiber reinforced composites. Compos Struct. 2024;339:118142. doi:10.1016/j.compstruct.2024.118142.
99. Ahangar M, Saeedifar M. The effect of plasma treatment on the mode II interlaminar fracture toughness of glass/epoxy laminates. Theor Appl Fract Mech. 2023;127(5):104093. doi:10.1016/j.tafmec.2023.104093.
100. Hosseini SB, Gaff M, Li H, Hui D. Effect of fiber treatment on physical and mechanical properties of natural fiber-reinforced composites: a review. Rev Adv Mater Sci. 2023;62(1):20230131. doi:10.1515/rams-2023-0131.
101. Maji P, Pal D. Surface functionalization process: its advantages and disadvantages. Nanocellulose A Biopolym Biomed Appl. 2024:141–57. doi:10.1002/9781394172825.ch6.
102. Bilge K, Papila M. Interlayer toughening mechanisms of composite materials. In: Toughening mechanisms in composite materials. Amsterdam, The Netherlands: Elsevier; 2015. p. 263–94. doi:10.1016/b978-1-78242-279-2.00010-x.
103. Di Boon Y, Joshi SC. A review of methods for improving interlaminar interfaces and fracture toughness of laminated composites. Mater Today Commun. 2020;22:100830. doi:10.1016/j.mtcomm.2019.100830.

104. Ramji A, Xu Y, Yasaee M, Grasso M, Webb P. Influence of veil interleave distribution on the delamination resistance of cross-ply CFRP laminates under low velocity impact. Int J Impact Eng. 2021;157:103997. doi:10.1016/j.ijimpeng.2021.103997.
105. Mohammadi R, Akrami R, Assaad M, Imran A, Fotouhi M. Comparative analysis of delamination resistance in CFRP laminates interleaved by thermoplastic nanoparticle: evaluating toughening mechanisms in modes I and II. Compos Part C Open Access. 2024;15(16):100518. doi:10.1016/j.jcomc.2024.100518.
106. Kazemi H, Salamat-Talab M, Ghanbari D. On the interlaminar properties of ENF specimens of glass/epoxy composites incorporated novel hybrid electrospun interlayers. Polym Compos. 2025;46(16):14688–706. doi:10.1002/pc.30080.
107. Kheirkhah Barzoki P, Rezadoust AM, Latifi M, Saghafi H. The experimental and numerical study on the effect of PVB nanofiber mat thickness on interlaminar fracture toughness of glass/phenolic composites. Eng Fract Mech. 2018;194:145–53. doi:10.1016/j.engfracmech.2018.03.027.
108. Salimi-Mofrad H, Rahbar Ranji A, Saghafi H. Effect of electrospun PA66 nanofibrous mat thickness on mode-II fracture toughness using acoustic emission (AE) with data clustering technique. Theor Appl Fract Mech. 2023;124:103788. doi:10.1016/j.tafmec.2023.103788.
109. Cheng C, Zhang C, Zhou J, Jiang M, Sun Z, Zhou S, et al. Improving the interlaminar toughness of the carbon fiber/epoxy composites via interleaved with polyethersulfone porous films. Compos Sci Technol. 2019;183:107827. doi:10.1016/j.compscitech.2019.107827.
110. Bahmani M, Nosraty H, Mirdehghan SA, Varkiani SMH. Investigating the interlaminar fracture toughness of glass fiber/epoxy composites modified by polypropylene spunbond nonwoven fabric interlayers. Fibres Polym. 2024;25(3):1061–73. doi:10.1007/s12221-023-00466-4.
111. Li Z, Li J. Effects of number of carbon nanotube film layers on the interlaminar fracture properties of its based composites. Diam Relat Mater. 2024;148(3):111413. doi:10.1016/j.diamond.2024.111413.
112. Shan FL, Gu YZ, Li M, Liu YN, Zhang ZG. Effect of deposited carbon nanotubes on interlaminar properties of carbon fiber-reinforced epoxy composites using a developed spraying processing. Polym Compos. 2013;34(1):41–50. doi:10.1002/pc.22375.
113. Liu Y, Wang GD, Shen Y, Blackie E, He L. Mode-II fracture toughness of carbon fiber reinforced polymer composites interleaved with polyethersulfone (PES)/carbon nanotubes (CNTs). Compos Struct. 2023;320(8):117214. doi:10.1016/j.compstruct.2023.117214.
114. Zhang Y, An X, Zhao G, Jia H, Qiao Y, Gu H, et al. Multi-scale "core-sheath" structure of electrospun veils to enhance the interlaminar fracture toughness and in-plane properties of CF/poly(phthalazinone ether ketone) laminates. Compos Sci Technol. 2024;252:110612. doi:10.1016/j.compscitech.2024.110612.
115. Beylergil B, Duman V. Enhancing Mode-I and Mode-II fracture toughness of carbon fiber/epoxy laminated composites using 3D-printed polyamide interlayers. Proc Inst Mech Eng Part L J Mater Des Appl. 2024;238(3):578–91. doi:10.1177/14644207231198961.
116. Salamat-Talab M, Kazemi H. On the improving interlaminar fracture toughness of ENF composites based on additively manufactured interlayer: new approach. Theor Appl Fract Mech. 2025;138(6):104952. doi:10.1016/j.tafmec.2025.104952.
117. Zhang Y, Zhao H, Ou Y, Zhang H, Yao X, Mao D. Polyamide mesh as an effective toughening interlayer for GFRP composites: insights into fracture behavior and mechanisms. Adv Compos Hybrid Mater. 2025;8(4):283. doi:10.1007/s42114-025-01365-3.
118. Hassanzadeh-Aghdam MK, Mahmoodi MJ, Jamali J, Ansari R. A new micromechanical method for the analysis of thermal conductivities of unidirectional fiber/CNT-reinforced polymer hybrid nanocomposites. Compos Part B Eng. 2019;175(1):107137. doi:10.1016/j.compositesb.2019.107137.
119. Chang MS. An investigation on the dynamic behavior and thermal properties of MWCNTs/FRP laminate composites. J Reinf Plast Compos. 2010;29(24):3593–9. doi:10.1177/0731684410379510.
120. Iijima S. Helical microtubules of graphitic carbon. Nature. 1991;354(6348):56–8. doi:10.1038/354056a0.
121. Zhang XH, Zhang ZH, Xu WJ, Chen FC, Deng JR, Deng X. Toughening of cycloaliphatic epoxy resin by multiwalled carbon nanotubes. J Appl Polym Sci. 2008;110(3):1351–7. doi:10.1002/app.28590.

122. Ahmadi-Moghadam B, Sharafimasooleh M, Shadlou S, Taheri F. Effect of functionalization of graphene nanoplatelets on the mechanical response of graphene/epoxy composites. Mater Des (1980–2015). 2015;66:142–9. doi:10.1016/j.matdes.2014.10.047.
123. Mefford CH, Qiao Y, Salviato M. Failure behavior and scaling of graphene nanocomposites. Compos Struct. 2017;176(5):961–72. doi:10.1016/j.compstruct.2017.06.013.
124. Akhavan-Safar A, Salamat-Talab M, Delzendehrooy F, Barbosa AQ, da Silva LFM. Mode II fracture energy of laminated composites enhanced with micro-cork particles. J Braz Soc Mech Sci Eng. 2021;43(11):490. doi:10.1007/s40430-021-03220-0.
125. Liu Y, Zou A, Wang GD, Han C, Blackie E. Enhancing interlaminar fracture toughness of CFRP laminates with hybrid carbon nanotube/graphene oxide fillers. Diam Relat Mater. 2022;128:109285. doi:10.1016/j.diamond.2022.109285.
126. Soyugüzel T, Mecitoğlu Z, Kaftelen-Odabaşı H. Experimental and numerical investigation on the mode I and mode II interlaminar fracture toughness of nitrogen-doped reduced graphene oxide reinforced composites. Theor Appl Fract Mech. 2023;128:104103. doi:10.1016/j.tafmec.2023.104103.
127. Spearing SM, Evans AG. The role of fiber bridging in the delamination resistance of fiber-reinforced composites. Acta Metall Mater. 1992;40(9):2191–9. doi:10.1016/0956-7151(92)90137-4.
128. Sadeghalvaad M, Dabiri E, Zahmatkesh S, Afsharimoghadam P. Improved curing conditions and mechanical/chemical properties of nitrile butadiene rubber composites reinforced with carbon based nanofillers. J Nanostructures. 2019;9(3):453–67. doi:10.22052/JNS.2019.03.007.
129. Srivastava VK, Gries T, Veit D, Quadflieg T, Mohr B, Kolloch M. Effect of nanomaterial on mode I and mode II interlaminar fracture toughness of woven carbon fabric reinforced polymer composites. Eng Fract Mech. 2017;180(5):73–86. doi:10.1016/j.engfracmech.2017.05.030.
130. Daemi A, Reza Hamzeloo S, Refahi Oskouei A. On the interlaminar mode II fracture toughness evaluation of glass Fiber/Epoxy composites with cotton and kenaf natural fibers utilizing acoustic emission features. Compos Struct. 2025;351:118591. doi:10.1016/j.compstruct.2024.118591.
131. Salamat-Talab M, Shokrieh MM, Mohaghegh M. On the R-curve and cohesive law of glass/epoxy end-Notch flexure specimens with 0// θ interface fiber angles. Polym Test. 2021;93:106992. doi:10.1016/j.polymertesting.2020.106992.
132. Zhao G, Zhang X, Qiang W, Zhang X. Enhancing the interlaminar toughness and impact resistance of CFRP using MWCNTs and core-shell rubber synergistic strategy. Thin Walled Struct. 2025;212(1):113146. doi:10.1016/j.tws.2025.113146.
133. Lai J, Yu Y, Zhang X, Qiang W, Zhang X. Interlaminar fracture toughness and impact resistance of carbon fiber reinforced composite with magnetic aligned CNTs. Compos Part B Eng. 2025;291(2):112008. doi:10.1016/j.compositesb.2024.112008.
134. Hu B, Han W, Hu K, Yang F, Duan L, Jia H. The influence of CNF/SiO_2/SCF additives on interlaminar toughening of glass fiber/epoxy laminates. Polym Compos. 2026;47(7):6283–301. doi:10.1002/pc.70557.
135. Jia J, Du X, Chen C, Sun X, Mai YW, Kim JK. 3D network graphene interlayer for excellent interlaminar toughness and strength in fiber reinforced composites. Carbon. 2015;95(6):978–86. doi:10.1016/j.carbon.2015.09.001.
136. Jiao W, Niu G, Bai D, Zheng Y, Wang H, Liu Y. Interlaminar toughness of carbon fiber/epoxy laminates interleaved by nanofibrous veils: from molecular structure to macroscopic properties. Compos Sci Technol. 2025;267(5):111205. doi:10.1016/j.compscitech.2025.111205.
137. Lan B, Liu Y, Mo S, He M, Zhai L, Fan L. Interlaminar fracture behavior of carbon fiber/polyimide composites toughened by interleaving thermoplastic polyimide fiber veils. Materials. 2021;14(10):2695. doi:10.3390/ma14102695.
138. Shin YC, Lee WI, Kim HS. Mode II interlaminar fracture toughness of carbon nanotubes/epoxy film-interleaved carbon fiber composites. Compos Struct. 2020;236:111808. doi:10.1016/j.compstruct.2019.111808.
139. Chen X, Zhang Y, Qiao Y, Zhang E, Zhao W, Jian X, et al. Construction of micro–nanostructure for interlayer reinforcement and toughening of carbon fiber/poly(phthalazinone ether sulfone ketone) with coaxially spun

polyimide/polyvinylpyrrolidone–carbon nanotube core–shell fibers after stepwise etching. Compos Part A Appl Sci Manuf. 2025;199:109222. doi:10.1016/j.compositesa.2025.109222.
140. Shao K, Zhang X, Lin L, Shen S, Zheng T, Wang X, et al. Investigation of interlaminar toughening properties in carbon fiber composites using wet veil formation of short-cut aramid fibers. Polym Compos. 2025;46(9):8015–24. doi:10.1002/pc.29473.
141. Khan SU, Kim JK. Improved interlaminar shear properties of multiscale carbon fiber composites with bucky paper interleaves made from carbon nanofibers. Carbon. 2012;50(14):5265–77. doi:10.1016/j.carbon.2012.07.011.
142. Zhang Z, Fu K, Li Y. Improved interlaminar fracture toughness of carbon fiber/epoxy composites with a multiscale cellulose fiber interlayer. Compos Commun. 2021;27(14):100898. doi:10.1016/j.coco.2021.100898.
143. Too DK, Kumar S, Kim YH. Fracture toughness and failure behavior of CF/epoxy composites interleaved with melt-infused PET, PEI, and PEEK film. Polym Compos. 2024;45(13):12307–24. doi:10.1002/pc.28637.
144. Lyashenko T, Lerman N, Wolf A, Harel H, Marom G. Improved mode II delamination fracture toughness of composite materials by selective placement of protein-surface treated CNT. Compos Sci Technol. 2013;85(12):29–35. doi:10.1016/j.compscitech.2013.06.001.
145. Wang G, Yu M, Wang M, Liu X, Zhang H, He L. Study of interlaminar fracture toughness and flexural properties of carbon fibre composites reinforced with polyethersulfone/graphene oxide films. Compos Commun. 2024;51(132):102051. doi:10.1016/j.coco.2024.102051.
146. Du X, Liu HY, Xu F, Zeng Y, Mai YW. Flame synthesis of carbon nanotubes onto carbon fiber woven fabric and improvement of interlaminar toughness of composite laminates. Compos Sci Technol. 2014;101(23):159–66. doi:10.1016/j.compscitech.2014.07.011.
147. Song X, Gao J, Zheng N, Zhou H, Mai YW. Interlaminar toughening in carbon fiber/epoxy composites interleaved with CNT-decorated polycaprolactone nanofibers. Compos Commun. 2021;24(3):100622. doi:10.1016/j.coco.2020.100622.
148. Hamer S, Leibovich H, Green A, Avrahami R, Zussman E, Siegmann A, et al. Mode I and Mode II fracture energy of MWCNT reinforced nanofibrilmats interleaved carbon/epoxy laminates. Compos Sci Technol. 2014;90(5):48–56. doi:10.1016/j.compscitech.2013.10.013.
149. Ma T, Sun Y, Yao J. Influence of carbon nanotubes/polyetherketone-cardo interlayer structure on mode II interlaminar fracture toughness of the interleaved carbon fiber reinforced epoxy composites. J Appl Polym Sci. 2022;139(30):e52671. doi:10.1002/app.52671.
150. Kazemi H, Salamat-Talab M, Ghanbari D. Investigating the mode II critical strain energy release rate of glass/epoxy laminated composites reinforced with polyvinyl alcohol interlayer. Iran J Manuf Eng. 2024;11(3):51–62.
151. Lu T, Xue L, Ning H, Wu X, Ding Z, Hu N, et al. Optimizing thickness and interlayer placement of electrospun TPU nanofibrous membranes for enhanced interlaminar performance and impact resistance in CFRP laminates. Polym Compos. 2026;47(1):646–61. doi:10.1002/pc.70172.
152. Wang Y, Shen W, Chen L, Zhu L, Natsuki T. Interlaminar fracture toughness of carbon/epoxy composites laminates toughened by short carbon fiber. Polym Compos. 2023;44(8):5261–71. doi:10.1002/pc.27488.
153. Saghafi H, Zucchelli A, Palazzetti R, Minak G. The effect of interleaved composite nanofibrous mats on delamination behavior of polymeric composite materials. Compos Struct. 2014;109(2):41–7. doi:10.1016/j.compstruct.2013.10.039.
154. Zheng N, Song Y, Lan M, Dong X, Zhou H, Gao J. Improved interlaminar property of carbon fiber/epoxy composites with polyurethane/RGO core-shell structure fibrous mat. Compos Commun. 2023;44:101748. doi:10.1016/j.coco.2023.101748.
155. Liu L, Huang ZM, Xu GY, Liang YM, Dong GH. Mode II interlaminar delamination of composite laminates incorporating with polymer ultrathin fibers. Polym Compos. 2008;29(3):285–92. doi:10.1002/pc.20367.
156. Zheng N, Huang Y, Liu HY, Gao J, Mai YW. Improvement of interlaminar fracture toughness in carbon fiber/epoxy composites with carbon nanotubes/polysulfone interleaves. Compos Sci Technol. 2017;140(1):8–15. doi:10.1016/j.compscitech.2016.12.017.

157. Yu M, Wu L, Xie W, Zhang O, Liu X, Ren M, et al. Improving interlaminar fracture toughness and compression after impact strength of carbon fiber reinforced epoxy composites by interleaving electrospinning polyethersulfone nanofiber. Polym Compos. 2025;46(6):5805–14. doi:10.1002/pc.29336.
158. Uppin VS, Shivakumar Gouda PS, Sridhar I, Umarfarooq MA, Edacherian A. Interleaving carbon-glass veils in glass epoxy composite for enhanced fracture toughness and interlaminar shear strength—a hybrid approach. Polym Compos. 2024;45(12):10654–65. doi:10.1002/pc.28498.
159. Narducci F, Lee KY, Pinho ST. Interface micro-texturing for interlaminar toughness tailoring: a film-casting technique. Compos Sci Technol. 2018;156(3):203–14. doi:10.1016/j.compscitech.2017.10.016.
160. Wang J, Pozegic TR, Xu Z, Nigmatullin R, Harniman RL, Eichhorn SJ. Cellulose nanocrystal-polyetherimide hybrid nanofibrous interleaves for enhanced interlaminar fracture toughness of carbon fibre/epoxy composites. Compos Sci Technol. 2019;182:107744. doi:10.1016/j.compscitech.2019.107744.